AEDC-TR-78-8

cy.2

SUPPORT INTERFERENCE ON AN OGIVE-CYLINDER MODEL AT HIGH ANGLE OF ATTACK IN TRANSONIC FLOW

M. C. Altstatt and W. E. Dietz, Jr.
ARO, Inc., a Sverdrup Corporation Company

PROPULSION WIND TUNNEL FACILITY
ARNOLD ENGINEERING DEVELOPMENT CENTER
AIR FORCE SYSTEMS COMMAND
ARNOLD AIR FORCE STATION, TENNESSEE 37389

March 1978

Final Report for Period 1 July 1976 - 30 September 1977

Prepared for

ARNOLD ENGINEERING DEVELOPMENT CENTER/DOTR
ARNOLD AIR FORCE STATION, TENNESSEE 37389

NOTICES

When U. S. Government drawings, specifications, or other data are used for any purpose other than a definitely related Government procurement operation, the Government thereby incurs no responsibility nor any obligation whatsoever, and the fact that the Government may have formulated, furnished, or in any way supplied the said drawings, specifications, or other data, is not to be regarded by implication or otherwise, or in any manner licensing the holder or any other person or corporation, or conveying any rights or permission to manufacture, use, or sell any patented invention that may in any way be related thereto.

Qualified users may obtain copies of this report from the Defense Documentation Center.

References to named commerical products in this report are not to be considered in any sense as an indorsement of the product by the United States Air Force or the Government.

This report has been reviewed by the Information Office (OI) and is releasable to the National Technical Information Service (NTIS). At NTIS, it will be available to the general public, including foreign nations.

APPROVAL STATEMENT

This report has been reviewed and approved.

Alexander F. Money

ALEXANDER F. MONEY
Project Manager, Research Division
Directorate of Test Engineering

Approved for publication:

FOR THE COMMANDER

Marion L. Laster

MARION L. LASTER
Director of Test Engineering
Deputy for Operations

REPORT DOCUMENTATION PAGE		READ INSTRUCTIONS BEFORE COMPLETING FORM
1 REPORT NUMBER AEDC-TR-78-8	2. GOVT ACCESSION NO.	3 RECIPIENT'S CATALOG NUMBER
4. TITLE (and Subtitle) SUPPORT INTERFERENCE ON AN OGIVE-CYLINDER MODEL AT HIGH ANGLE OF ATTACK IN TRANSONIC FLOW		5 TYPE OF REPORT & PERIOD COVERED Final Report, 1 July 1976 - 30 Sept 1977 6. PERFORMING ORG. REPORT NUMBER
7 AUTHOR(s) M. C. Altstatt and W. E. Dietz, ARO, Inc.		8 CONTRACT OR GRANT NUMBER(s)
9 PERFORMING ORGANIZATION NAME AND ADDRESS Arnold Engineering Development Center Air Force Systems Command Arnold Air Force Station, TN 37389		10 PROGRAM ELEMENT, PROJECT, TASK AREA & WORK UNIT NUMBERS Program Element 65807F
11. CONTROLLING OFFICE NAME AND ADDRESS Arnold Engineering Development Center (DOS) Air Force Systems Command Arnold Air Force Station, TN 37389		12 REPORT DATE March 1978 13. NUMBER OF PAGES 65
14 MONITORING AGENCY NAME & ADDRESS(if different from Controlling Office)		15. SECURITY CLASS. (of this report) UNCLASSIFIED 15a DECLASSIFICATION/DOWNGRADING SCHEDULE N/A

16 DISTRIBUTION STATEMENT (of this Report)

Approved for public release; distribution unlimited.

17. DISTRIBUTION STATEMENT (of the abstract entered in Block 20, if different from Report)

18. SUPPLEMENTARY NOTES

Available in DDC.

19 KEY WORDS (Continue on reverse side if necessary and identify by block number)

interference
walls
supports
wind tunnels
flow fields
sting supports
strut supports

20 ABSTRACT (Continue on reverse side if necessary and identify by block number)

A combined experimental and analytic study was conducted to determine the relative magnitude of the support and tunnel wall interferences on an ogive-cylinder model at a high angle of attack in transonic flow. The tests were conducted in the AEDC Aerodynamic Wind Tunnel (4T). The results indicate that the strut support causes large reductions in the normal force on the model, while the effect attributable to the sting support is much smaller. A correction procedure applied to the data to

DD FORM 1 JAN 73 1473 EDITION OF 1 NOV 65 IS OBSOLETE

20. ABSTRACT (Continued)

remove support interference gives consistent results. The test data, combined with an inviscid analytic study, indicate that the wall interference effects were negligible. Solutions obtained using two computational methods compare well with experimental results.

AFSC
Arnold AFS Tenn

PREFACE

The research reported herein was conducted by the Arnold Engineering Development Center (AEDC), Air Force Systems Command (AFSC), under Program Element 65807F. Results of this research were obtained by ARO, Inc., AEDC Division (a Sverdrup Corporation Company), operating contractor for the AEDC, AFSC, Arnold Air Force Station, Tennessee. The work was conducted under ARO Project Number P32A-K3A. The manuscript was submitted for publication on December 22, 1977.

CONTENTS

ILLUSTRATIONS

APPENDIXES

1.0 INTRODUCTION

Previous wind tunnel testing has shown that the force on an ogive-cylinder model at an angle of attack near 90 deg can vary considerably with the type of support used. For example, Ref. 1 shows differences between the normal force on sting- and strut-supported models that can exceed 25 percent at transonic Mach numbers. Also, sting-supported models generally exhibit much larger variations in normal force with Reynolds number than do the strut-supported models.

The results of previous studies, such as Ref. 2, indicate that the strut may act as a splitter plate, reducing the drag due to the wake. However, sting support interference, wall interference, and the effect of the model position relative to the main support system could also affect the measurements.

A combined experimental and analytic study was conducted to identify and determine the magnitude of the interference effects. The experimental program included a range of angle of attack from 66 to 100 deg, Mach numbers from 0.6 to 0.9, and Reynolds numbers from 2 to 4 million per foot. The analytic phase included a potential flow solution for the model with wind tunnel walls and computer solutions using two semi-empirical methods for the calculation of body force coefficients.

2.0 EXPERIMENTAL PROCEDURE

2.1 APPARATUS

2.1.1 Wind Tunnel

Testing was conducted in the AEDC Aerodynamic Wind Tunnel (4T), a continuous flow, variable density, transonic wind tunnel having a 4-ft square test section with perforated walls. The model supports were attached to the pitch sector, which has a pitch capability of 35 deg. A more complete description of the facility is given in Ref. 3.

2.1.2 Model Configurations

Figure 1a is a photograph of the model mounted on the sting support with the dummy strut added. Model dimensions are presented in Fig. 1b. All testing was accomplished with fixed boundary-layer transition. Two strips of No. 60 grit were applied longitudinally on the model, 30 deg to each side of the windward centerline.

The support configurations are shown in Fig. 2. The sting support configuration can be modified by adding a dummy strut or extending the boom to move the model closer to the wall. The strut support configuration can also be modified by the addition of a dummy sting.

2.2 TEST DESCRIPTION

2.2.1 Test Conditions

For each configuration, the model angle of attack was varied from 66 to 100 deg in 2-deg increments at Mach numbers of 0.6, 0.8, and 0.9 and Reynolds numbers of 2, 3, and 4 million per foot.

2.2.2 Measurements

Force measurements were obtained with an internal strain-gage balance. The normal-force coefficient, moment coefficient, and center-of-pressure location are presented in Appendix A. The uncertainty in the data is typically 2 to 3 percent and is never larger than the symbol size used.

Oil flow photographs were taken for the sting and sting with dummy strut configurations at angles of attack of 65 and 90 deg for the full range of Mach and Reynolds numbers for the test.

3.0 EXPERIMENTAL RESULTS

3.1 DATA SUMMARY

Normal-force coefficient, moment coefficient, and center-of-pressure location obtained in the wind tunnel are shown in Appendix A. A summary of the data is presented in this section to illustrate the support effects.

3.1.1 Strut and Sting Supports

The Reynolds number effect on the strut-supported model (Fig. 2a) was small, as shown in Fig. 3. The sting-supported model (Fig. 2b) exhibited higher normal force and more variation in normal force with Reynolds number (Fig. 4), especially at M = 0.6 and 0.8.

3.1.2 Sting Support with Dummy Strut

The normal-force coefficient on the sting-supported model (Fig. 2b) and the sting-supported model with dummy strut (Fig. 2c) are compared in Fig. 5a. The addition of the dummy strut caused a significant reduction in the normal-force coefficient, almost to the level of the normal-force coefficient on the strut-supported model (Fig. 5b).

3.1.3 Strut Support with Dummy Sting

The addition of the dummy sting (Fig. 2d) to the strut-supported model (Fig. 2a) produced an increase in normal-force coefficient. The effect was small, as shown in Fig. 6, but was present for all flow conditions.

3.1.4 Boom Extension

Extending the boom 6 in. to move the sting-supported model closer to the wall (Fig. 2b) resulted in no significant change in the force measured. Figure 7 shows the largest difference found. In addition to the test, a vortex lattice technique was applied to examine the wall interference effect and is presented in Appendix B. It was concluded that the wall interference on the model was insignificant.

3.2 INTERFERENCE EFFECTS

This discussion is concerned with support interference, since the test data and a vortex lattice investigation show that the wall interference is negligible.

3.2.1 Support Interference

The most significant interference effect shown by the data is caused by the strut support. The decrease in normal force on the model caused by the strut support is similar to the effect reported by Roshko (Ref. 2), where the crossflow drag on a cylinder is reduced by a splitter plate in the wake, preventing periodic vortex shedding. The oil flow photographs (Fig. 8) show that the flow near the surface of the model, including the location of the separation line, is not affected by the presence of the dummy strut. This supports the conclusion that the force reduction is a wake effect. Also, data from previous tests (Ref. 1) show that the normal force on a model with a strut attached at the nose and not immersed in the wake is in agreement with the force measured on a sting-supported model.

The increase in normal force caused by the dummy sting is approximately five percent and is consistent with an increase in effective model length of 10 to 20 percent (Refs. 1 and 4).

3.2.2 Interference Evaluation

Since sufficient data are available to define first-order effects, the support interference can be evaluated by the following equations:

$$\Delta C_{N1} = C_N \text{ (strut support)} - C_N \text{ (strut support with dummy sting)}$$

$$\Delta C_{N2} = C_N \text{ (sting support)} - C_N \text{ (sting support with dummy strut)}$$

where ΔC_{N1} represents the increment in the normal-force coefficient caused by the addition of the dummy sting to the strut-supported model and ΔC_{N2} is the increment caused by the dummy strut.

Assuming that the dummy sting correction is the same as the interference attributable to the sting support and the dummy strut correction is the same as the strut interference, then:

$$C_N \text{ (corrected, sting support)} = C_N \text{ (sting support)} - \Delta C_{N1}$$

$$C_N \text{ (corrected, strut support)} = C_N \text{ (strut support)} - \Delta C_{N2}$$

Where C_N (corrected, sting support) and C_N (corrected, strut support) are the normal-force coefficients of the model with the sting and strut interference removed. The difference between the two coefficients is a measure of the secondary effects.

Figure 9 shows curve fits to the data for the sting- and strut-supported configurations and the corrected curves. The area between the two curves for corrected coefficients is shaded for identification.

The close agreement between the two approximations for interference-free data demonstrates that the correction procedure gives good results.

The difference between the corrected sting support data and the corrected strut support data (shaded areas) corresponds closely to the difference between data for the sting-supported model with dummy strut and the strut-supported model with dummy sting. For example, comparing Fig. 9a with Fig. 10 indicates that the differences between the two interference-corrected curves can be attributed largely to secondary effects such as differences in geometry and tunnel position which exist for the two configurations that include the dummy supports.

4.0 ANALYTIC STUDY

4.1 SEMI-EMPIRICAL SOLUTIONS

Two methods for computing forces on missile-type bodies were used to obtain solutions for comparison with the experimental data. These methods, one by Jorgensen (Ref. 5) and the Computer-Aided Missile Synthesis Program (CAMS) by Tipping, et al. (Ref. 6) give semi-empirical solutions incorporating data from experimental studies.

4.1.1 Jorgensen's Method

A computer program was developed using Jorgensen's method, which combines potential and viscous flow components to determine the normal force on an ogive cylinder model. The equation used is as follows:

$$C_N = \frac{S_b}{S} \sin 2\alpha \cos \frac{\alpha}{2} + \eta C_{D_N} \frac{S_p}{S} \sin^2 \alpha$$

$$0 \leqslant \alpha \leqslant 180 \text{ deg}$$

Data from Jones, et al. (Ref. 7) and Goldstein (Ref. 4) are used for C_{D_N} and η.

4.1.2 Computer-Aided Missile Synthesis Program

A section of the CAMS program can be used to obtain forces and moments on a missile-type body. This program combines viscous and crossflow terms with extensive experimental data to provide solutions over a range of configurations and flow conditions, both subsonic and supersonic.

4.2 COMPARISONS WITH EXPERIMENTAL DATA

Solutions were obtained with both programs, and a comparison of these solutions with experimental data is shown in Fig. 11. The quantities plotted in Fig. 11a represent normal-force coefficients obtained for the sting-supported model and the strut-supported model from the Jorgensen program and the CAMS program. In addition, the normal-force coefficient for the ogive cylinder as corrected for support interference is shown in Figs. 11b and c. The interference-corrected curve is the average of the corrected sting support and corrected strut support data shown in Figs. 9a and c.

At M = 0.9 (Fig. 11a), the agreement between experimental and analytic results is good. At M = 0.6 (Figs. 11b and c), the difference between the analytic solutions and the interference-corrected data exceeds 10 percent due to the lack of reliable empirical inputs for the analytic solutions. The analytic solutions show no Reynolds number dependence at this Mach number.

5.0 CONCLUDING REMARKS

An investigation was conducted to evaluate sting interference, strut interference, and wall interference on an ogive-cylinder at high angle of attack in a transonic flow. The following conclusions were reached:

1. The major source of interference is the strut support. The strut acts as a splitter plate in the wake, reducing the crossflow drag and the Reynolds number effect.

2. The sting support also induces interference. The increase in normal-force coefficient caused by the sting support is consistent with an effective increase of 10 to 20 percent of model length.

3. The wall interference for this investigation is shown to be negligible both by the test results and by the vortex lattice analysis.

4. Corrections, based on measurements with and without the dummy sting and dummy strut can be applied to the data with consistent results.

5. Solutions obtained using the two semi-empirical computer methods compared well with the data at M = 0.9; however, errors were larger at M = 0.6, due to inadequate data inputs. Also, the computer solutions do not show Reynolds number dependence. Additional wind tunnel testing is needed to establish a data base in this range of Mach and Reynolds numbers.

REFERENCES

1. Baker, W. B. "An Aerodynamic Coefficient Prediction Technique for Slender Bodies with Low Aspect Ratio Fins at Transonic Mach Numbers and Angles of Attack to 180 Degrees." Ph.D. Dissertation, University of Tennessee, August 1976.

2. Roshko, Anatol. "Experiments on the Flow Past a Circular Cylinder at Very High Reynolds Number." Journal of Fluid Mechanics, Vol. 10, Pt 3, May 1961, pp. 345-356.

3. Test Facilities Handbook (Tenth Edition). "Propulsion Wind Tunnel Facility, Vol. 4." Arnold Engineering Development Center, May 1974.

4. Goldstein, Sidney. Modern Developments in Fluid Dynamics, Vol. 2, Oxford, the Clarendon Press, 1938.

5. Jorgensen, L. H. "Prediction of Static Aerodynamic Characteristics for Space-Shuttle-Like and Other Bodies at Angles of Attack from 0° to 180°." NASA TN D-6996, January 1973.

6. Tipping, Derrick E., et al. "Computer-Aided Missile Synthesis (CAMS)." OR 12,034, June 1972.

7. Jones, George W., Jr., Walker, Robert W., and Cincotta, Joseph J. "Aerodynamic Forces on a Stationary and Oscillating Circular Cylinder at High Reynolds Numbers." NASA TR R-300, February 1969.

8. Todd, D. C. "The AEDC Three-Dimensional, Potential Flow Computer Program." AEDC-TR-75-75, Vol. 1 (ADA021693), February 1976.

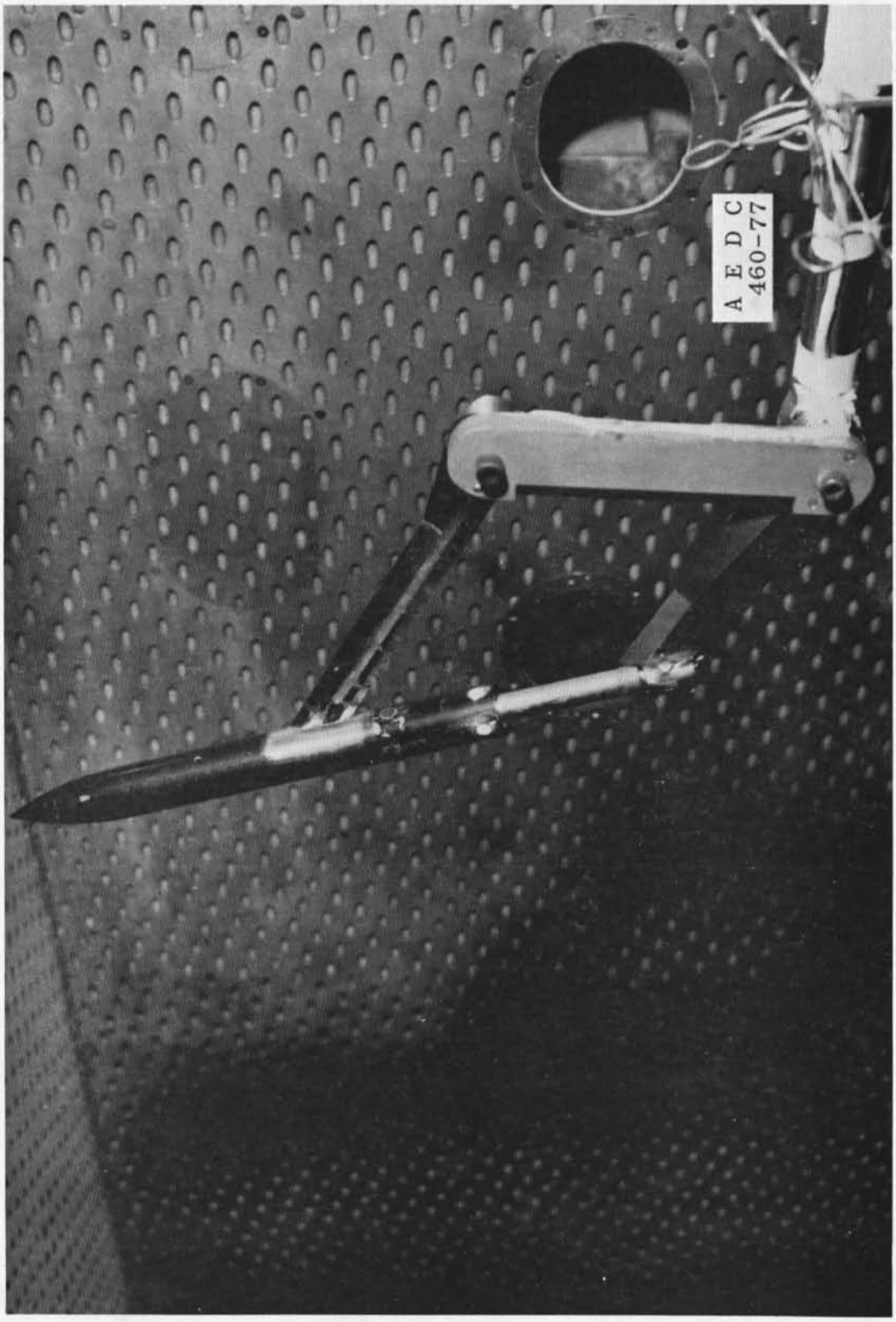

a. Sting-supported model with dummy strut

Figure 1. Model Description.

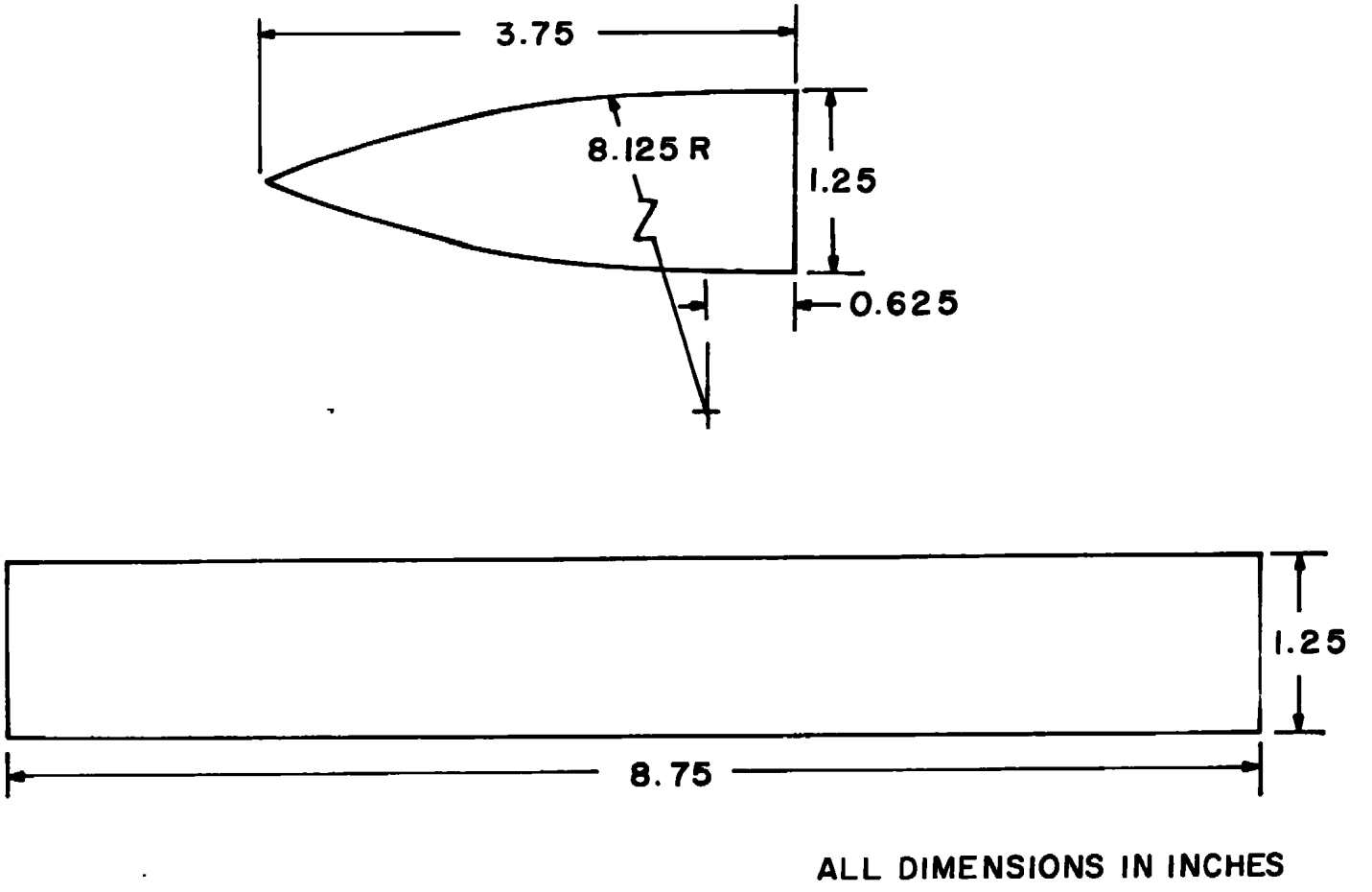

b. Model dimensions
Figure 1. Concluded.

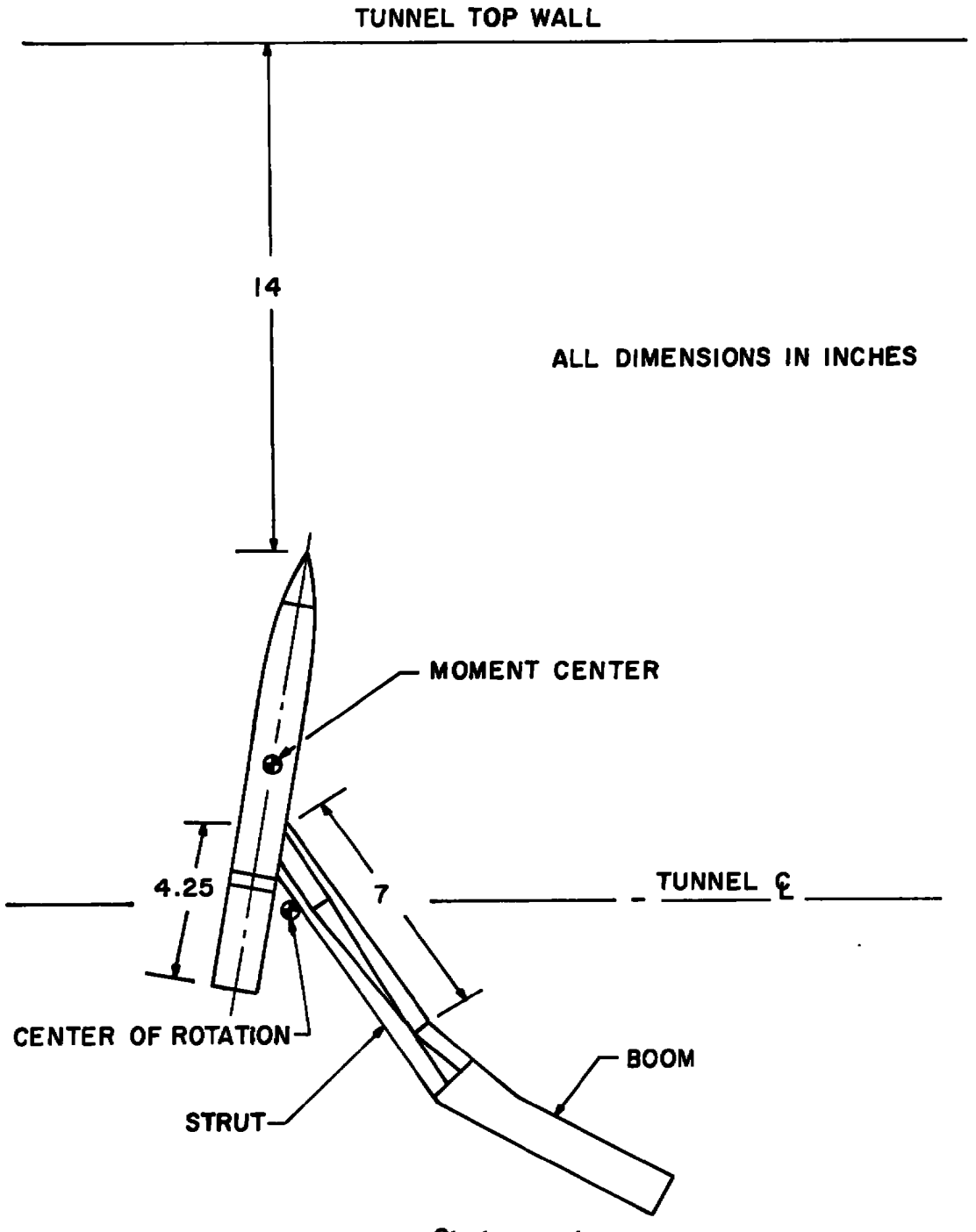

a. Strut support

Figure 2. Model support configurations.

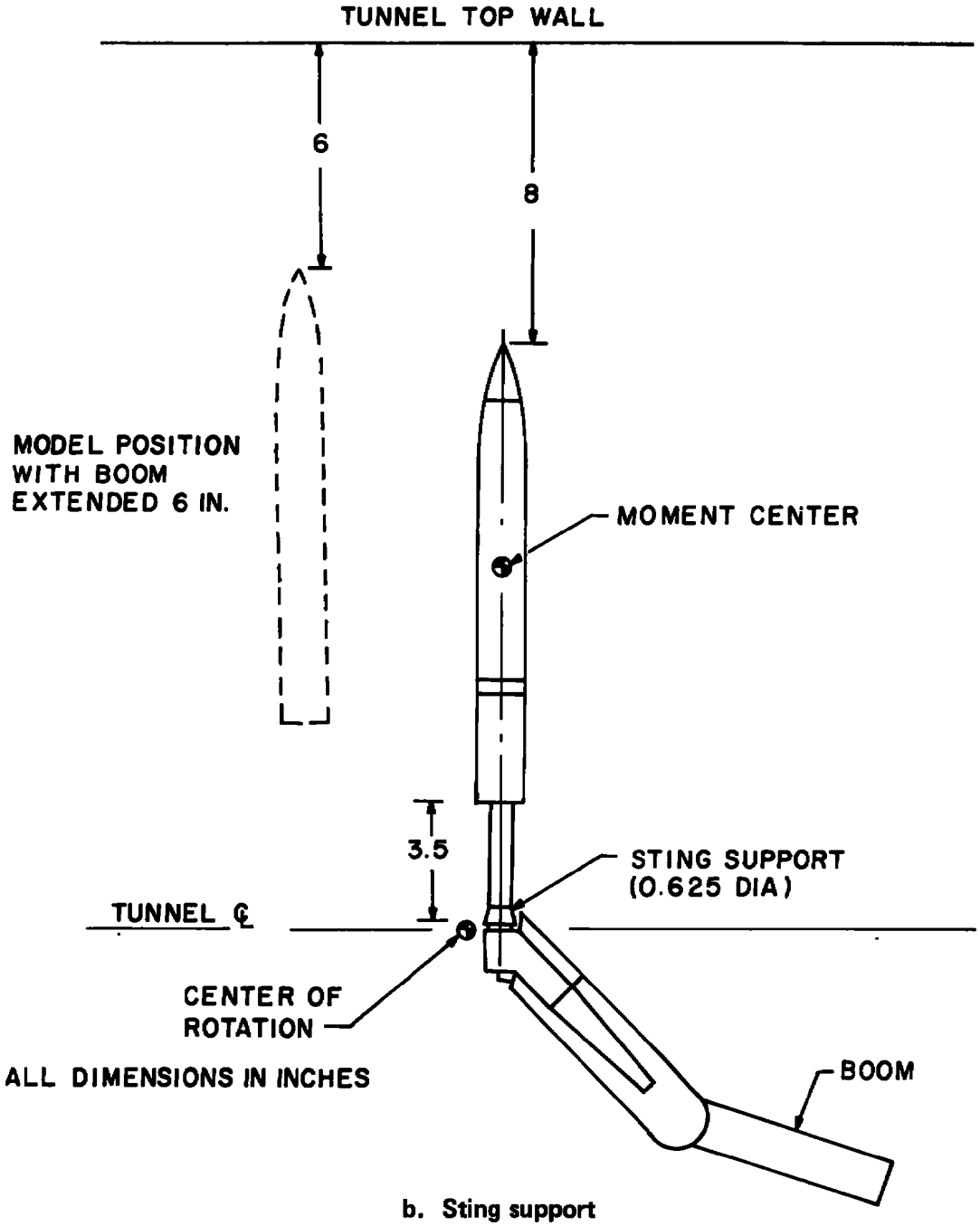

b. Sting support
Figure 2. Continued.

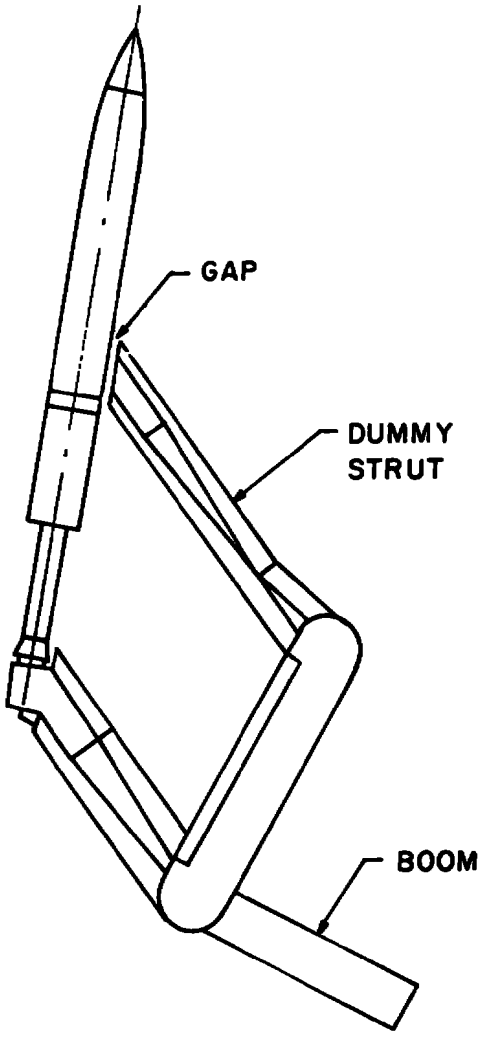

c. Sting support with dummy strut
Figure 2. Continued.

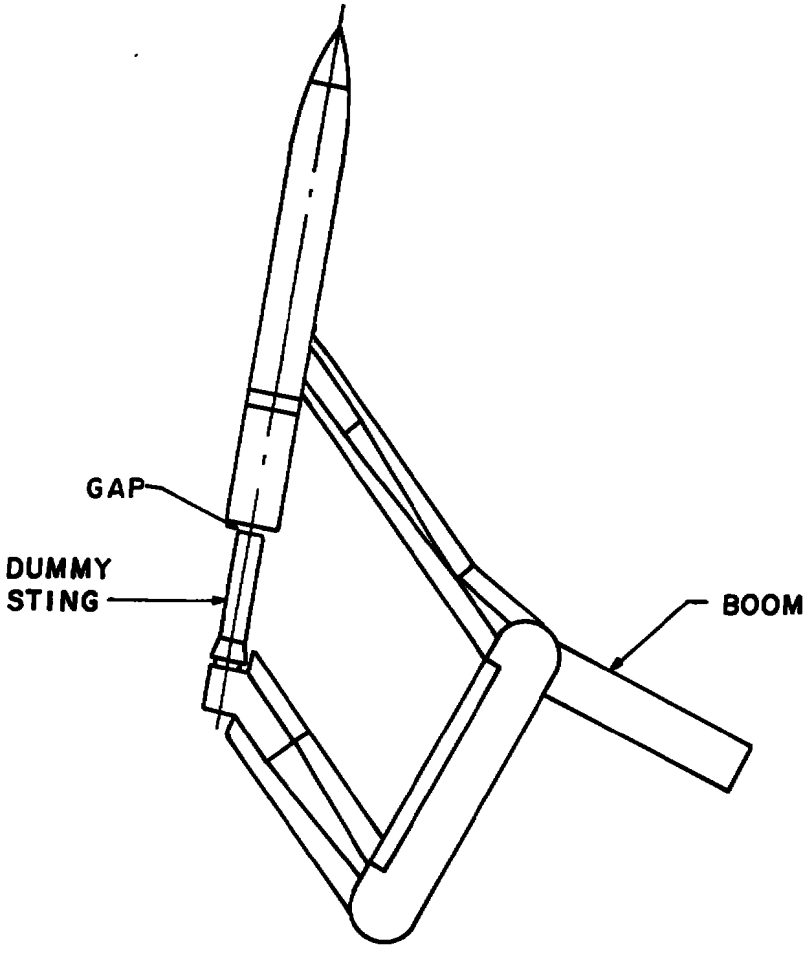

d. Strut support with dummy sting
Figure 2. Concluded.

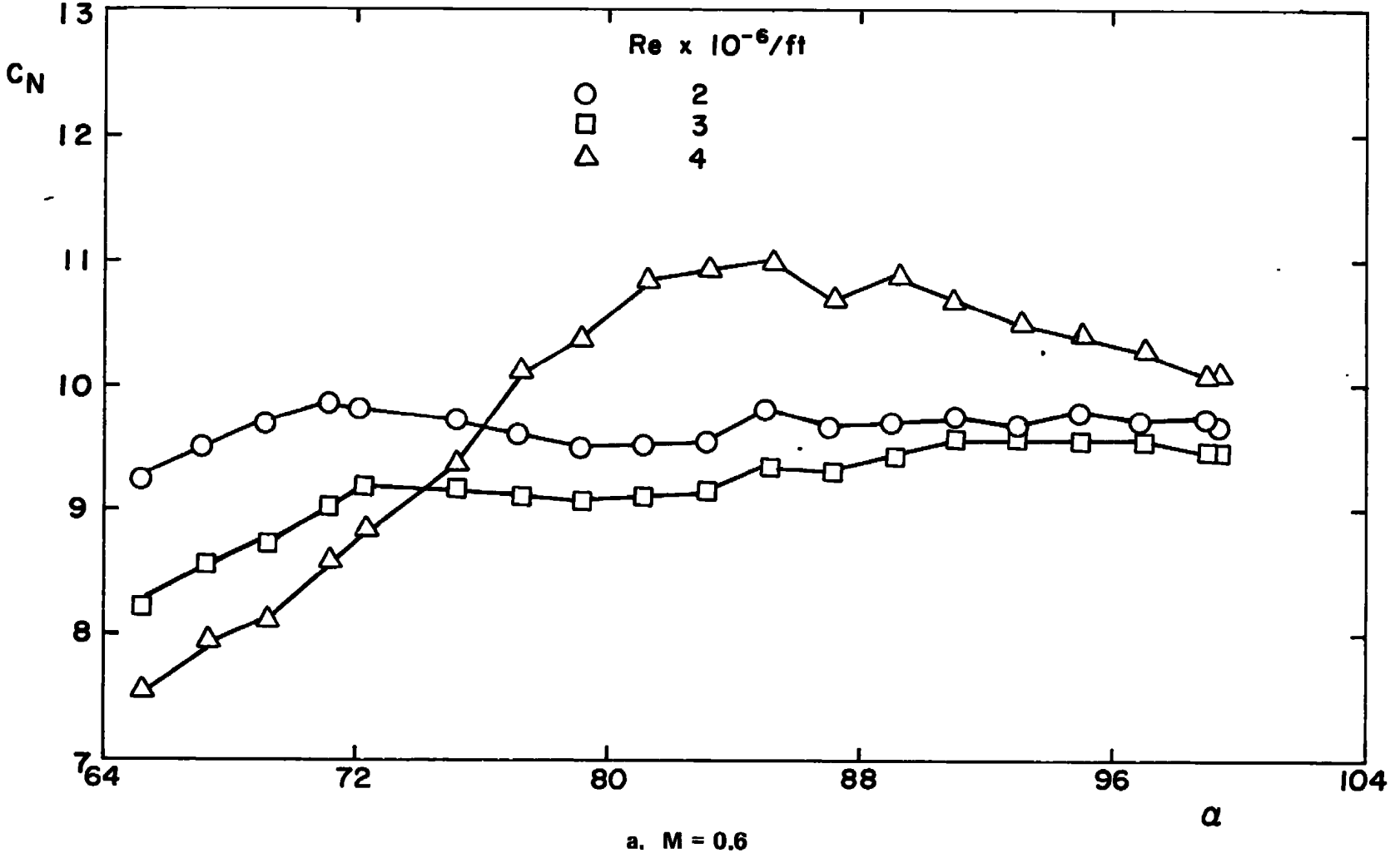

a. M = 0.6

Figure 3. Strut-supported model data.

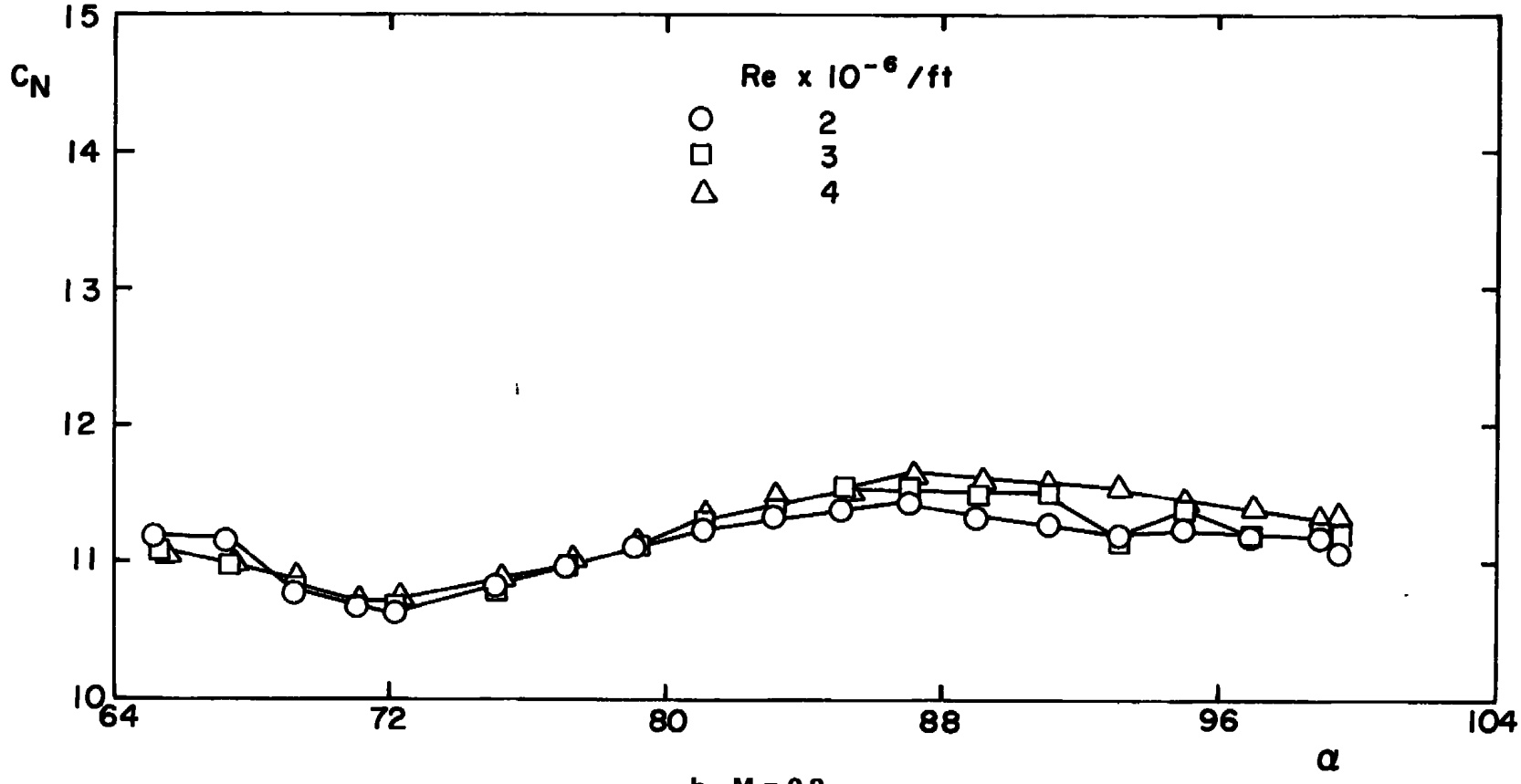

b. M = 0.8

Figure 3. Continued.

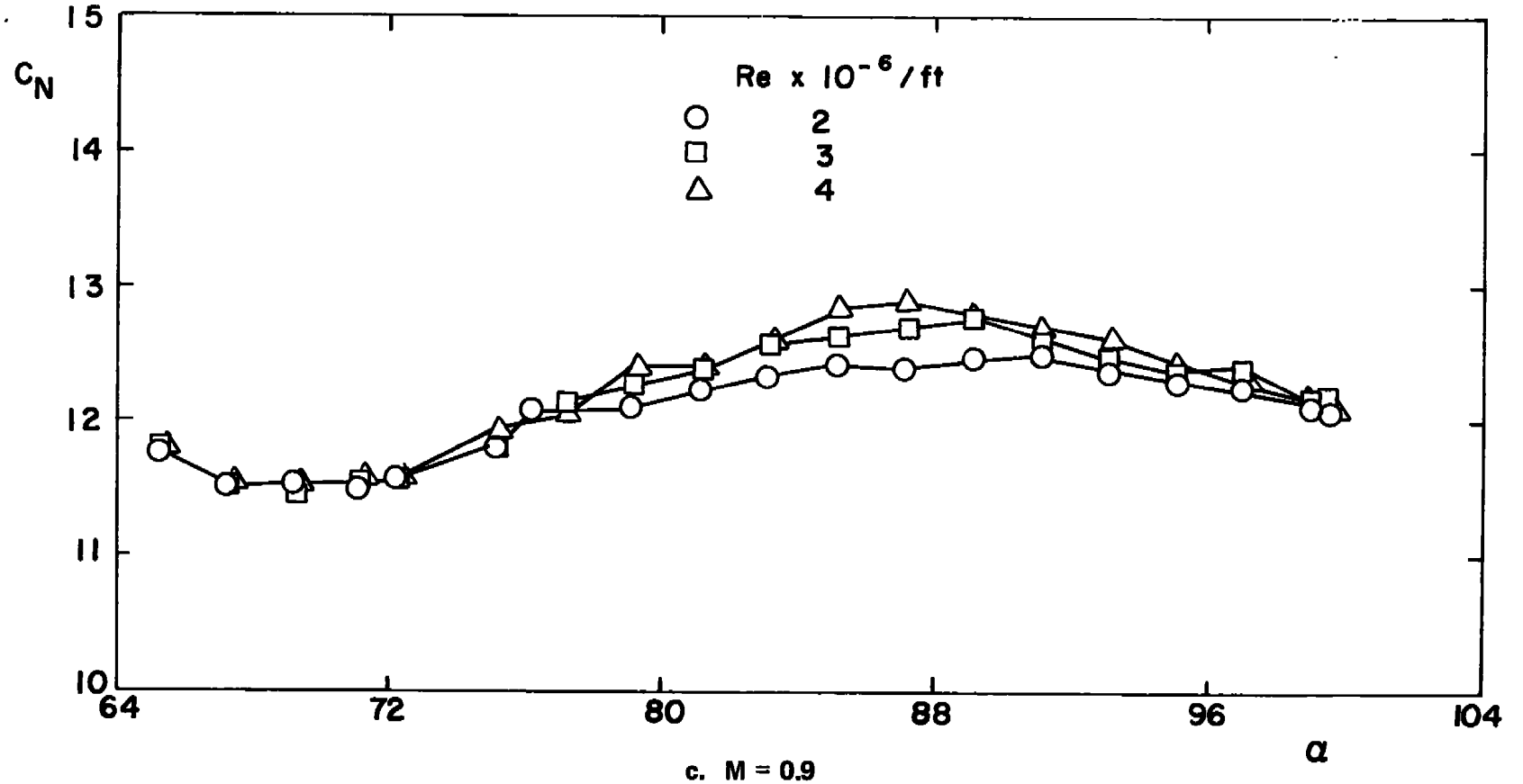

c. M = 0.9

Figure 3. Concluded.

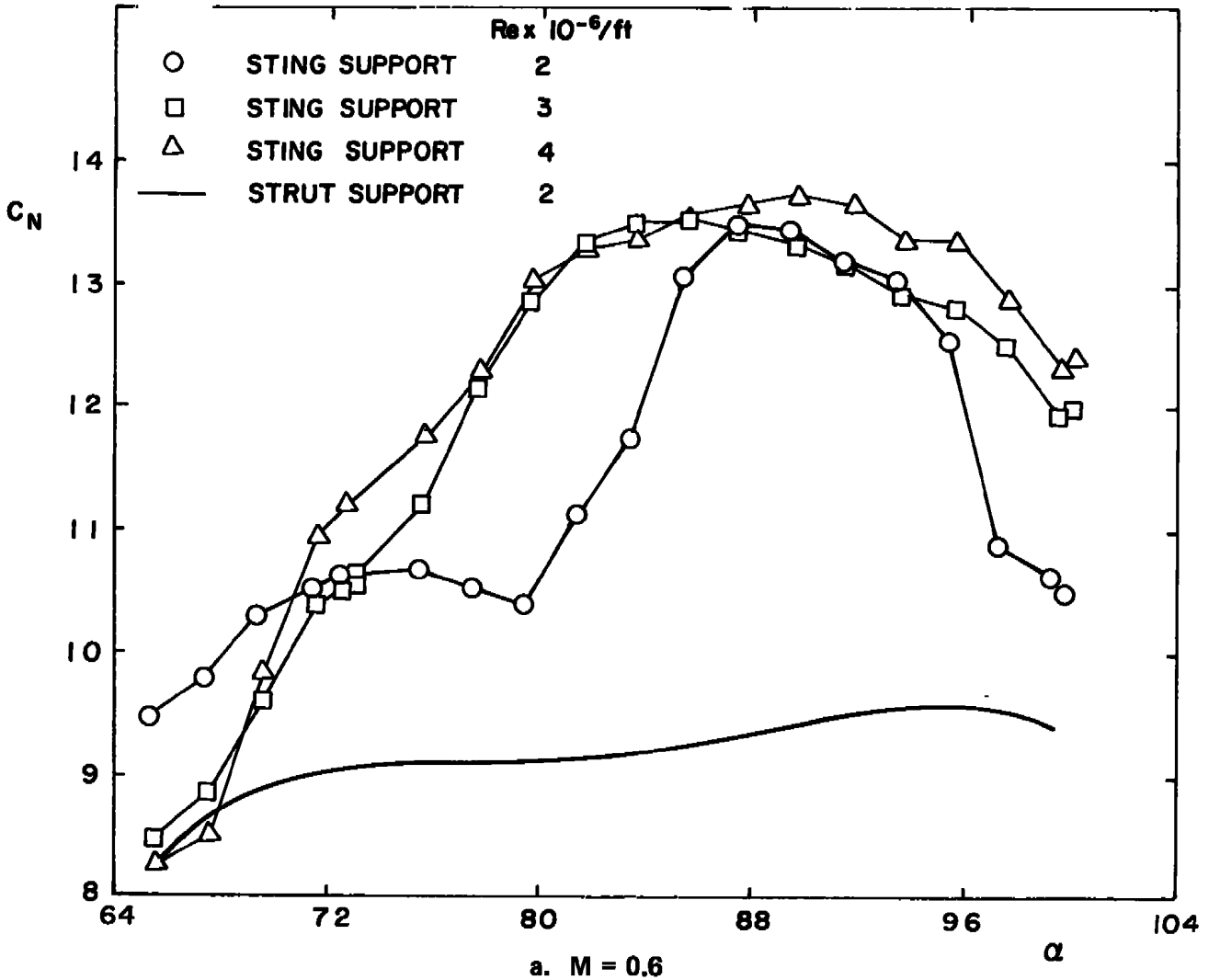

a. M = 0.6

Figure 4. Sting-supported model data.

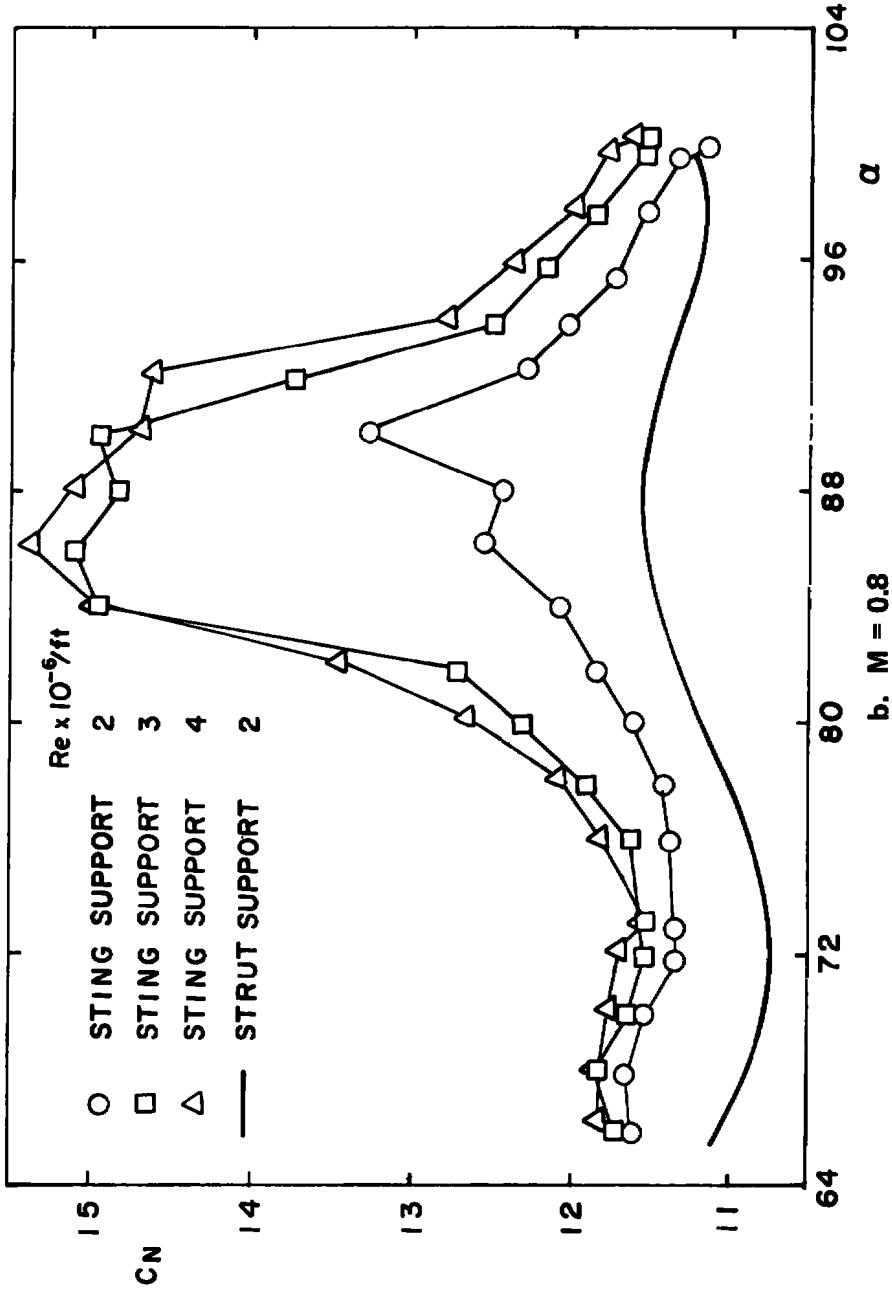

b. M = 0.8

Figure 4. Continued.

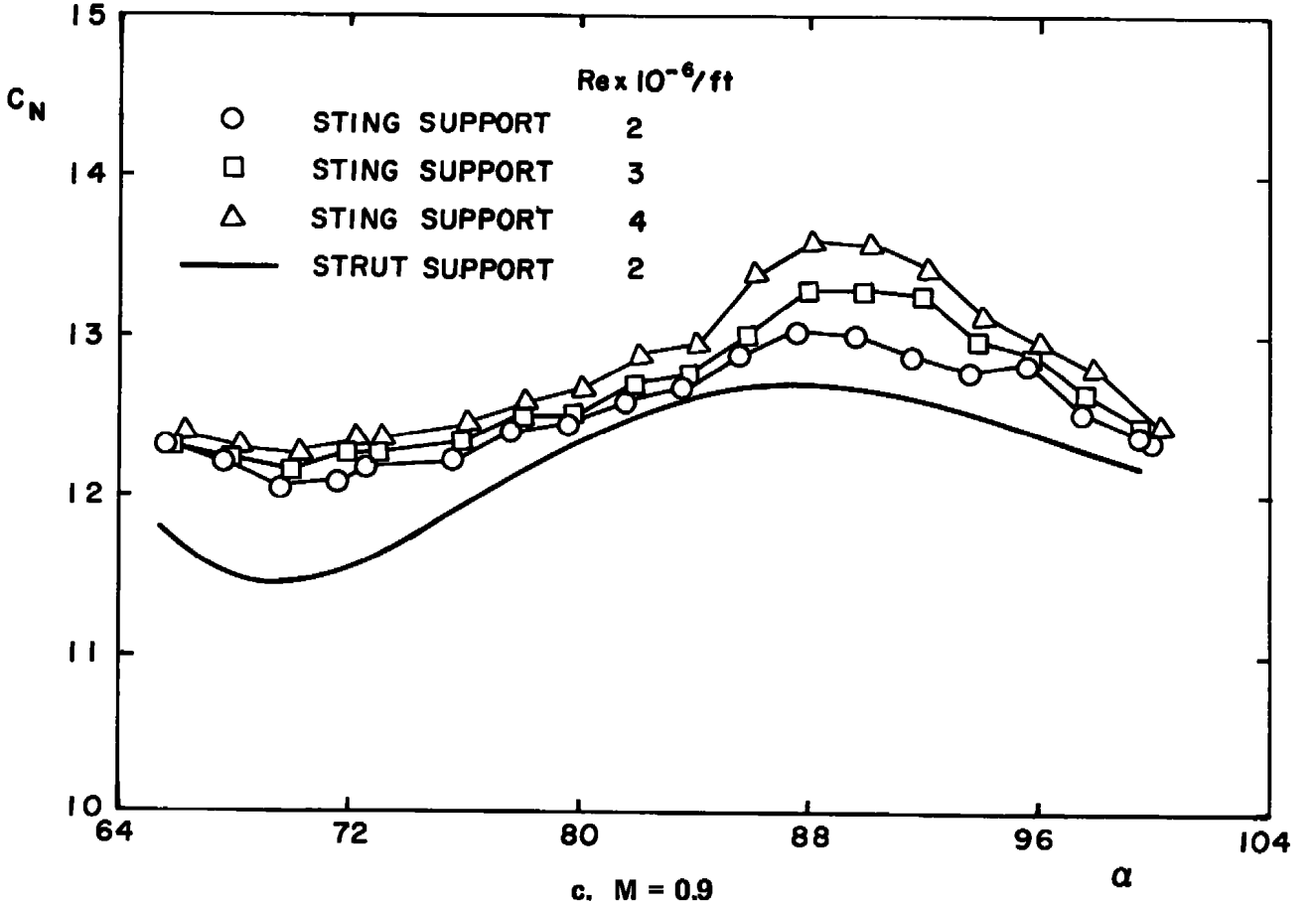

c. M = 0.9

Figure 4. Concluded.

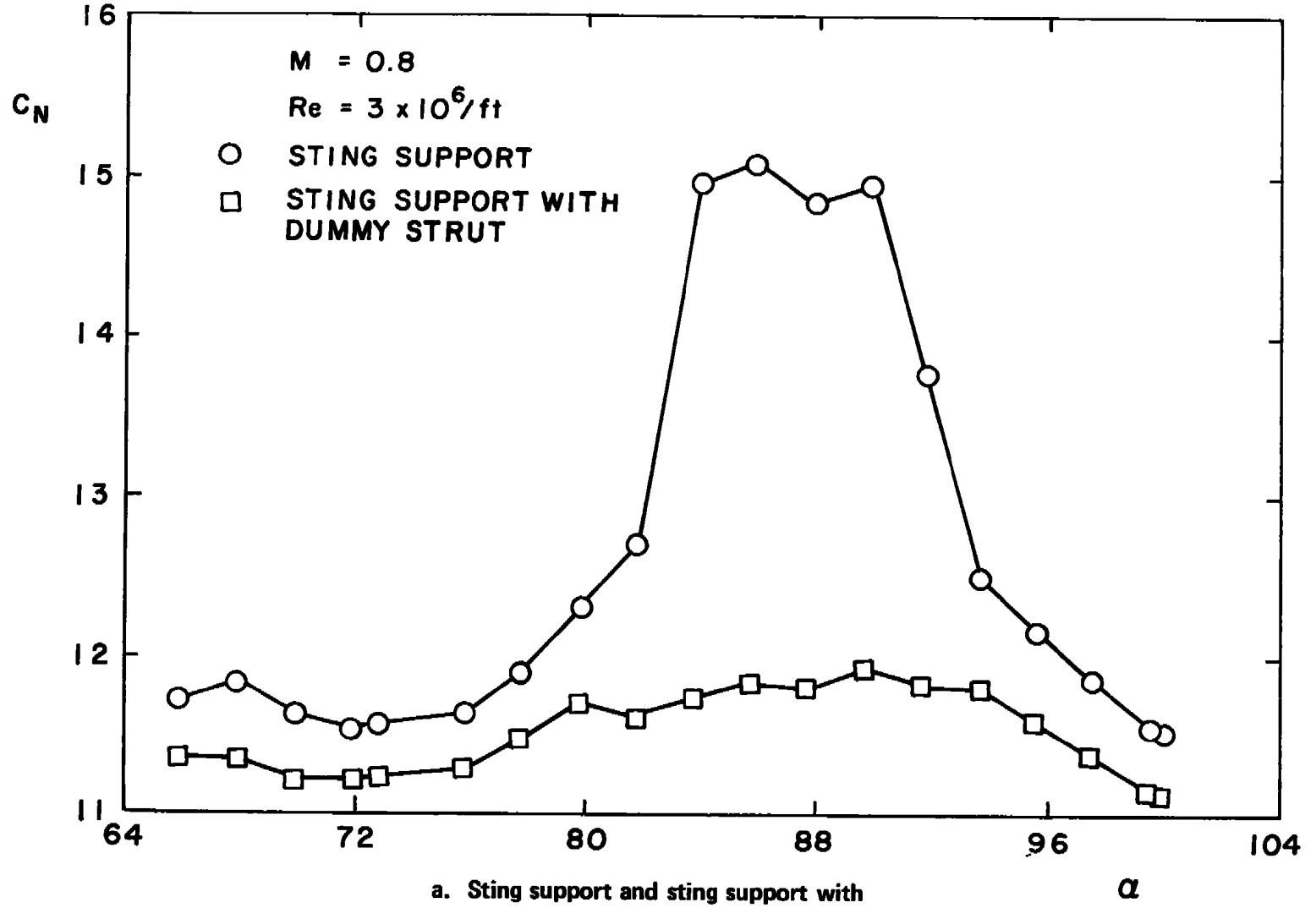

a. Sting support and sting support with dummy strut.

Figure 5. Dummy strut effects.

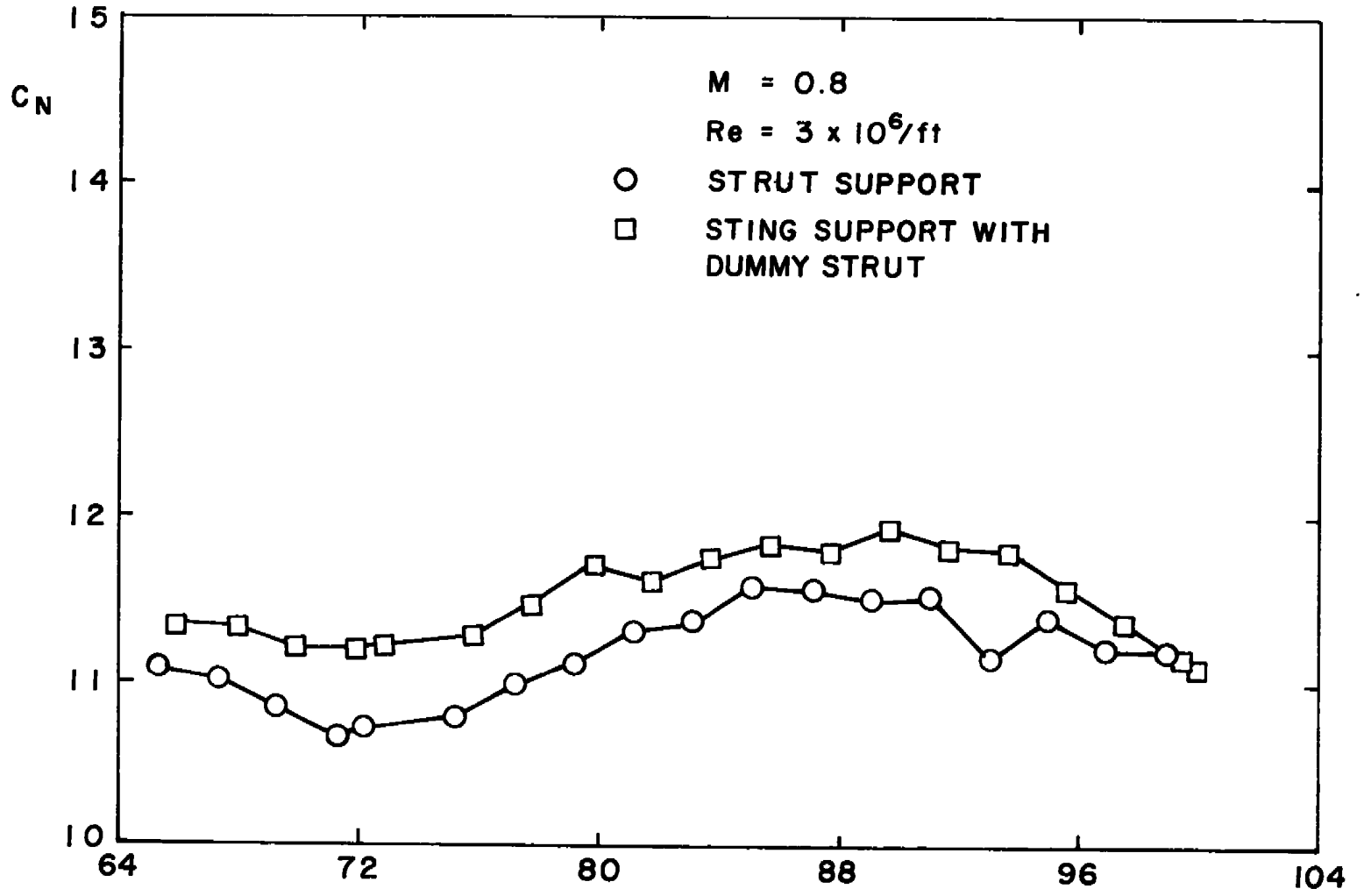

b. Strut support and sting support with dummy strut

Figure 5. Concluded.

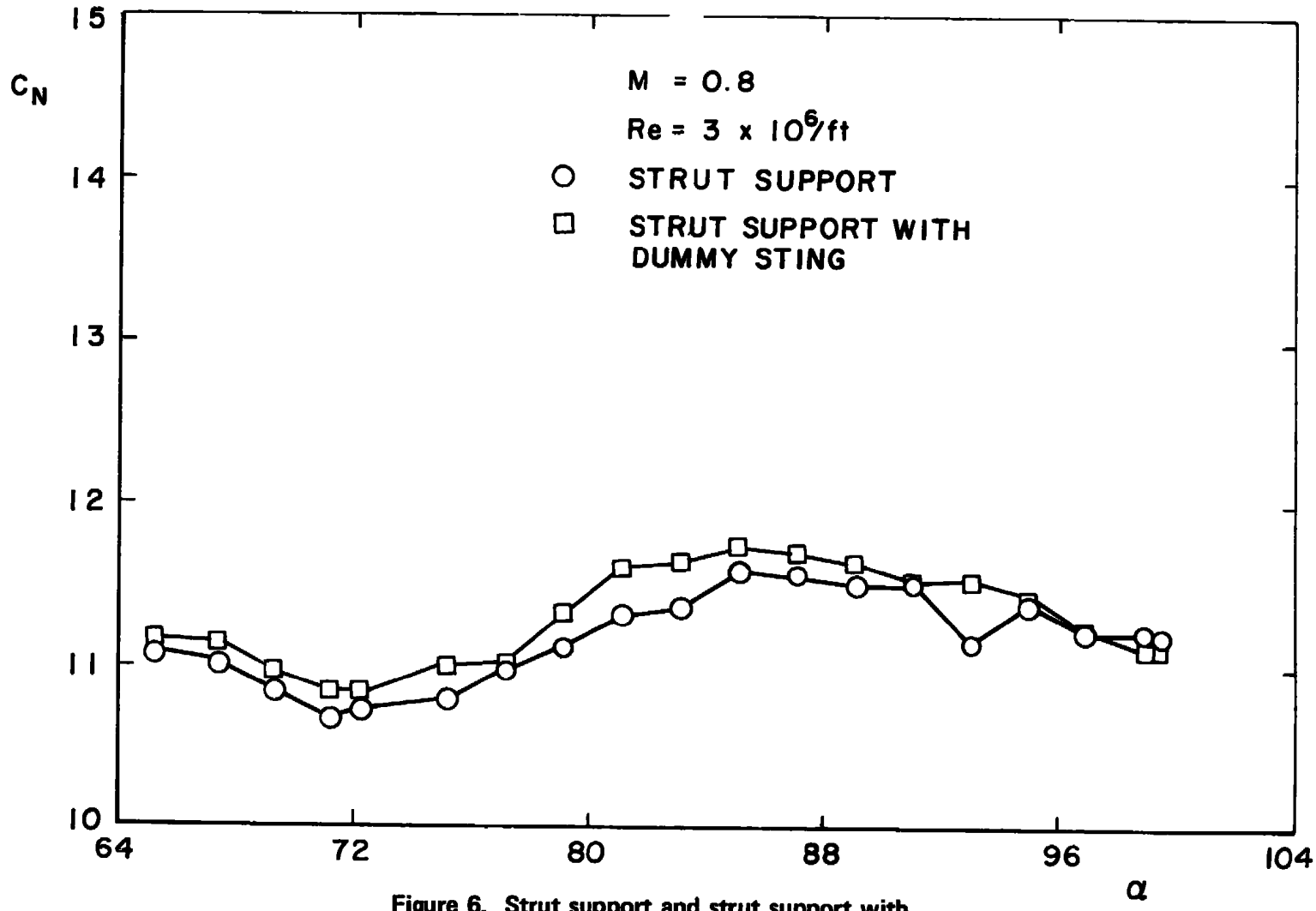

Figure 6. Strut support and strut support with dummy sting.

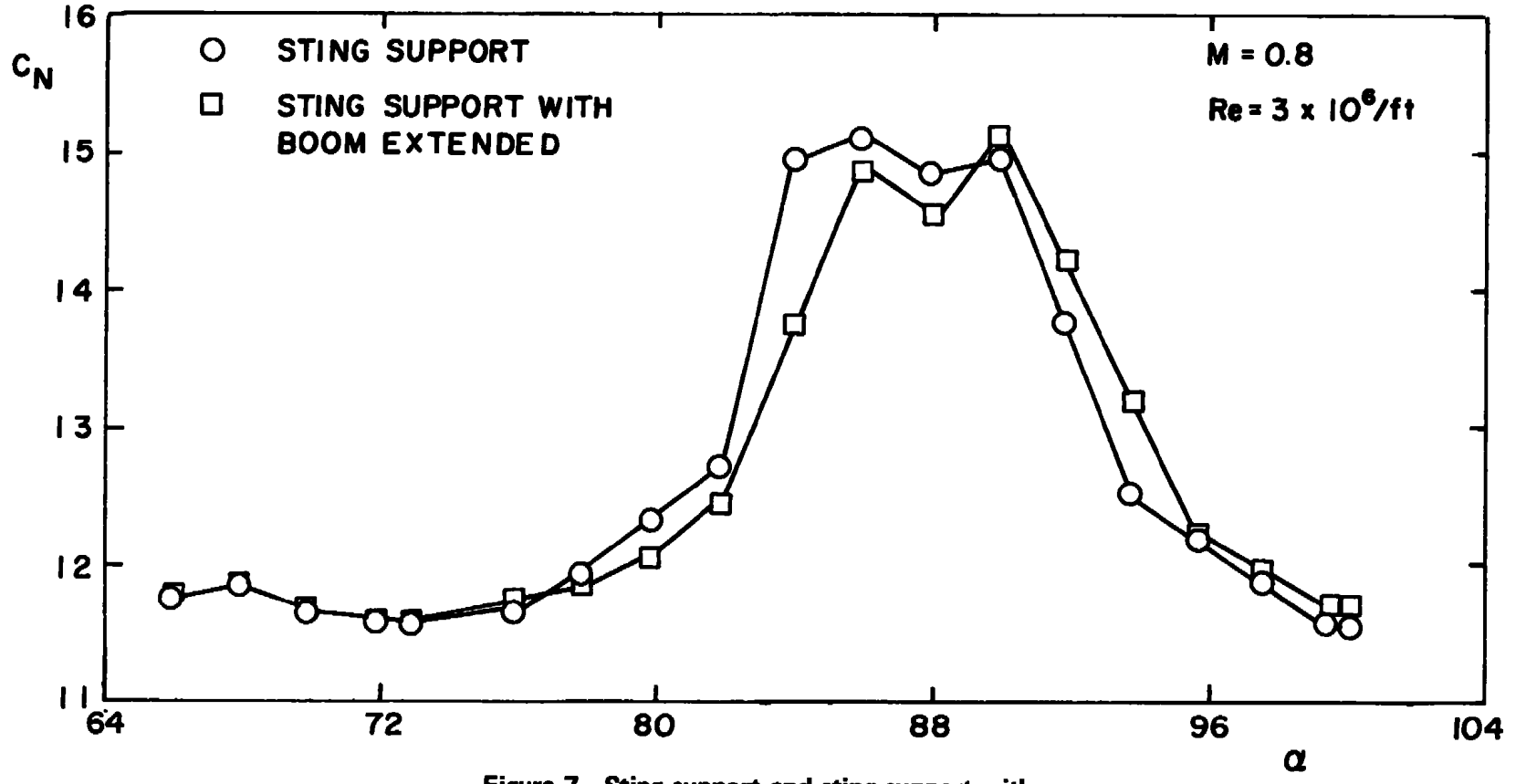

Figure 7. Sting support and sting support with boom extended.

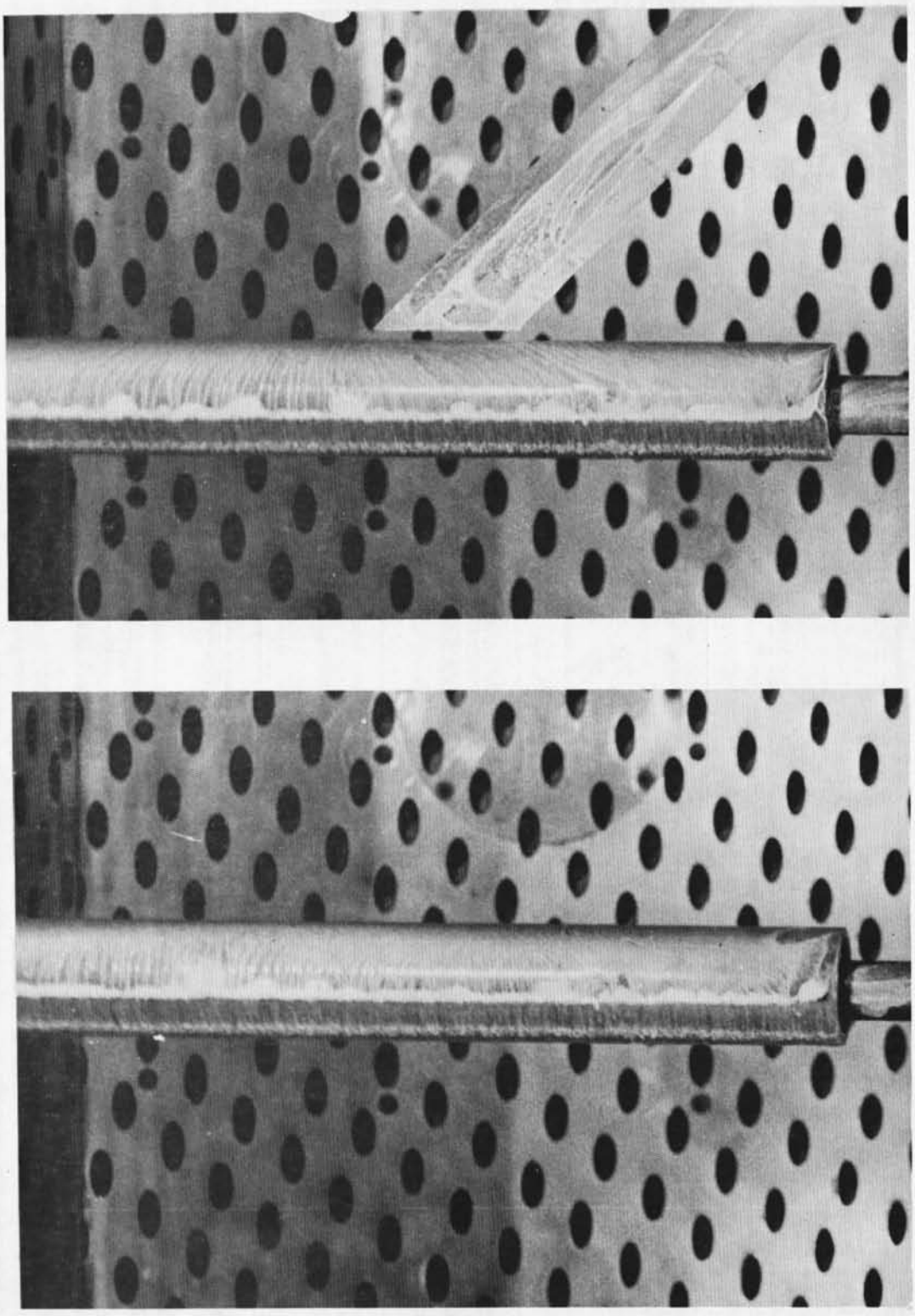

Figure 8. Oil flow photograph of sting-supported model and sting-supported model with dummy strut.

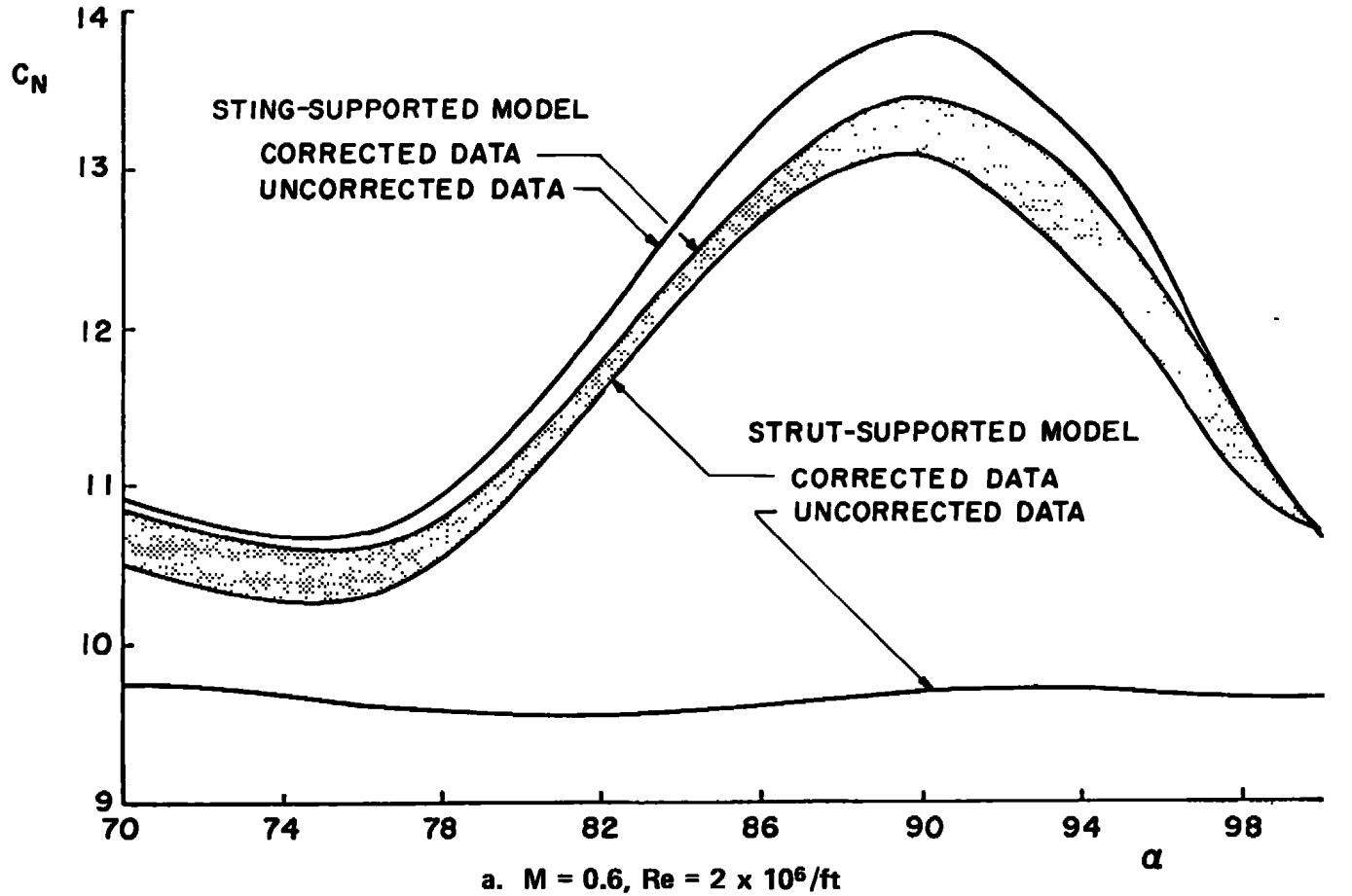

a. M = 0.6, Re = 2 x 10^6/ft

Figure 9. Interference corrections.

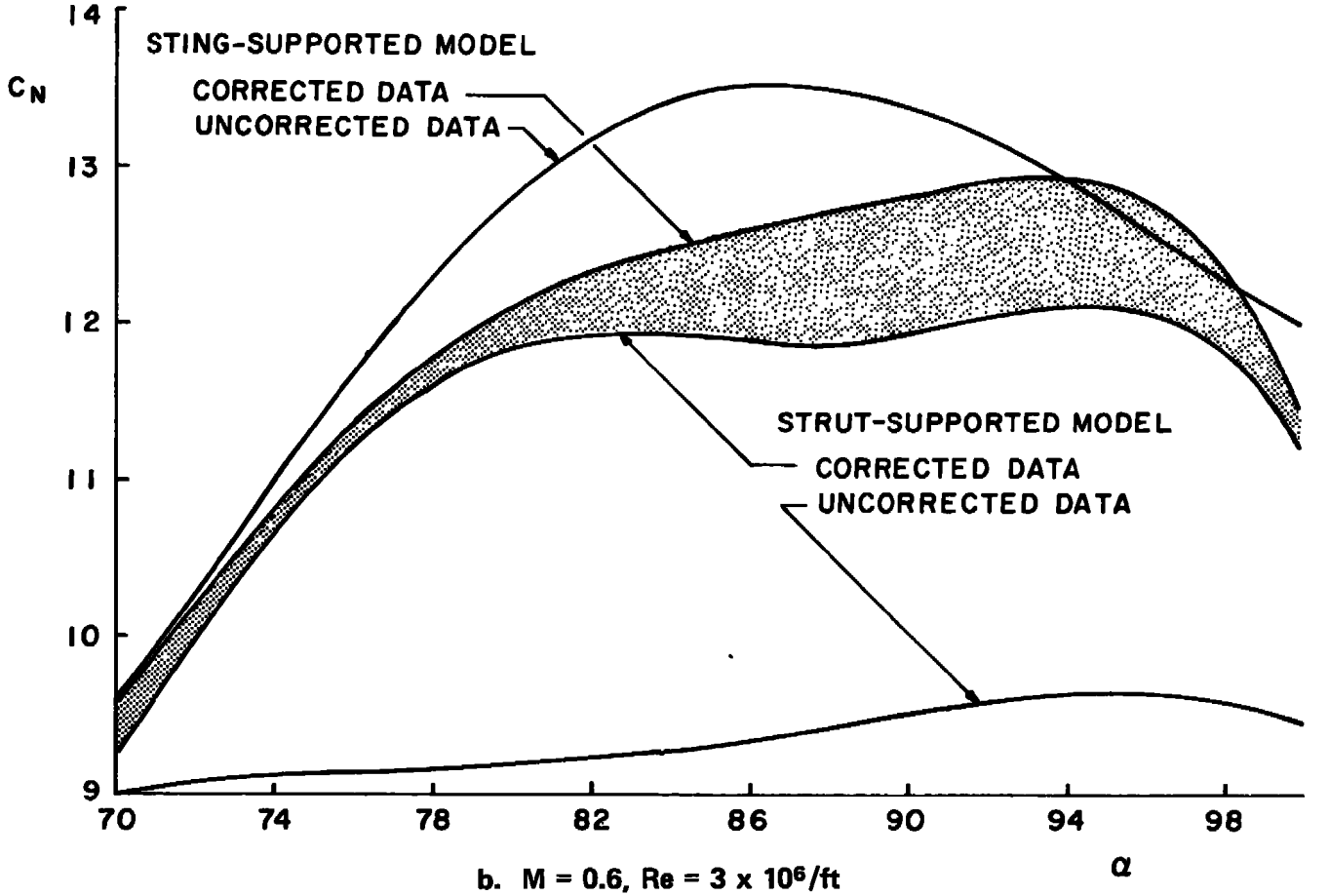

b. M = 0.6, Re = 3 x 10^6/ft

Figure 9. Continued.

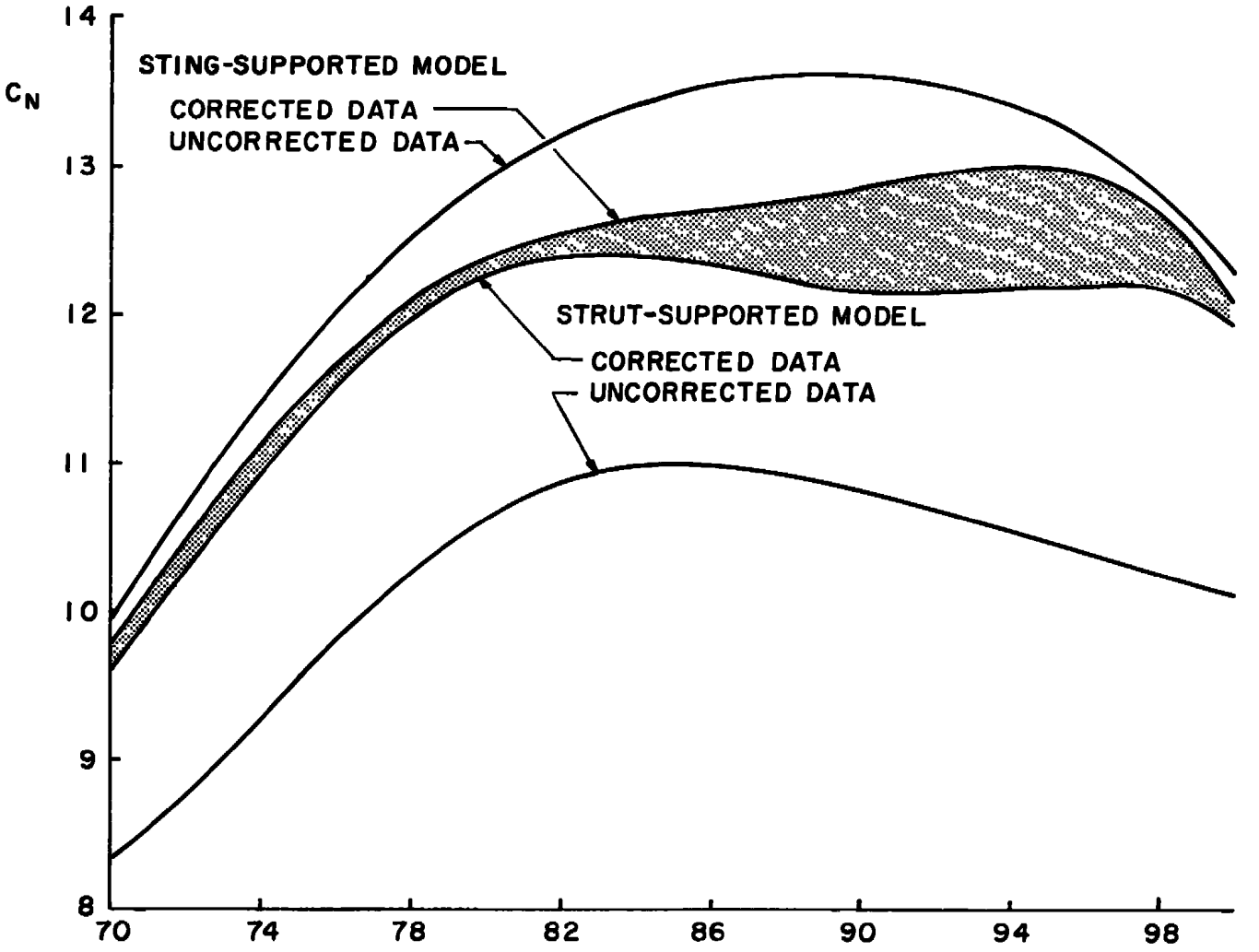

c. M = 0.6, Re = 4 x 10^6/ft

Figure 9. Continued.

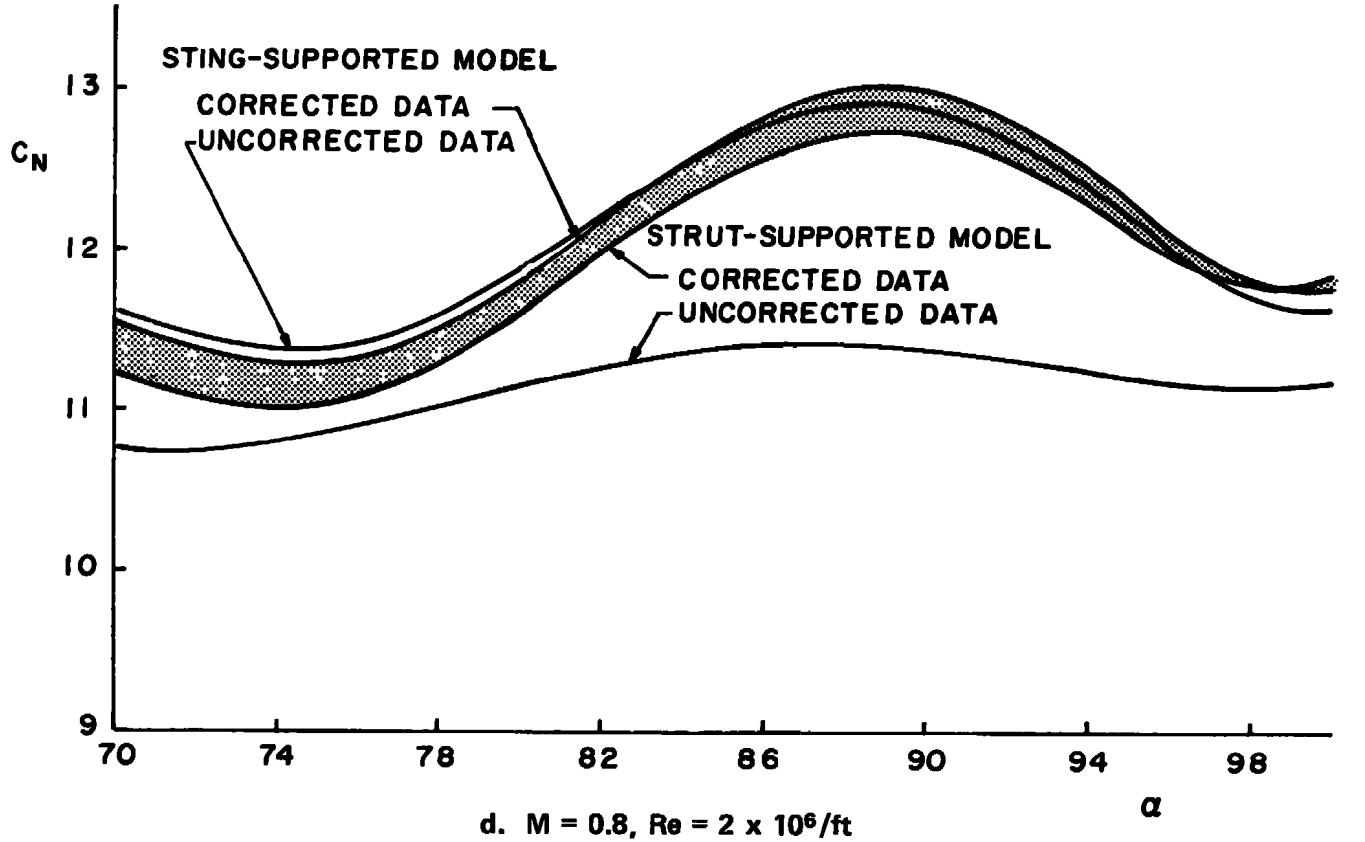

d. M = 0.8, Re = 2 x 10^6/ft

Figure 9. Continued.

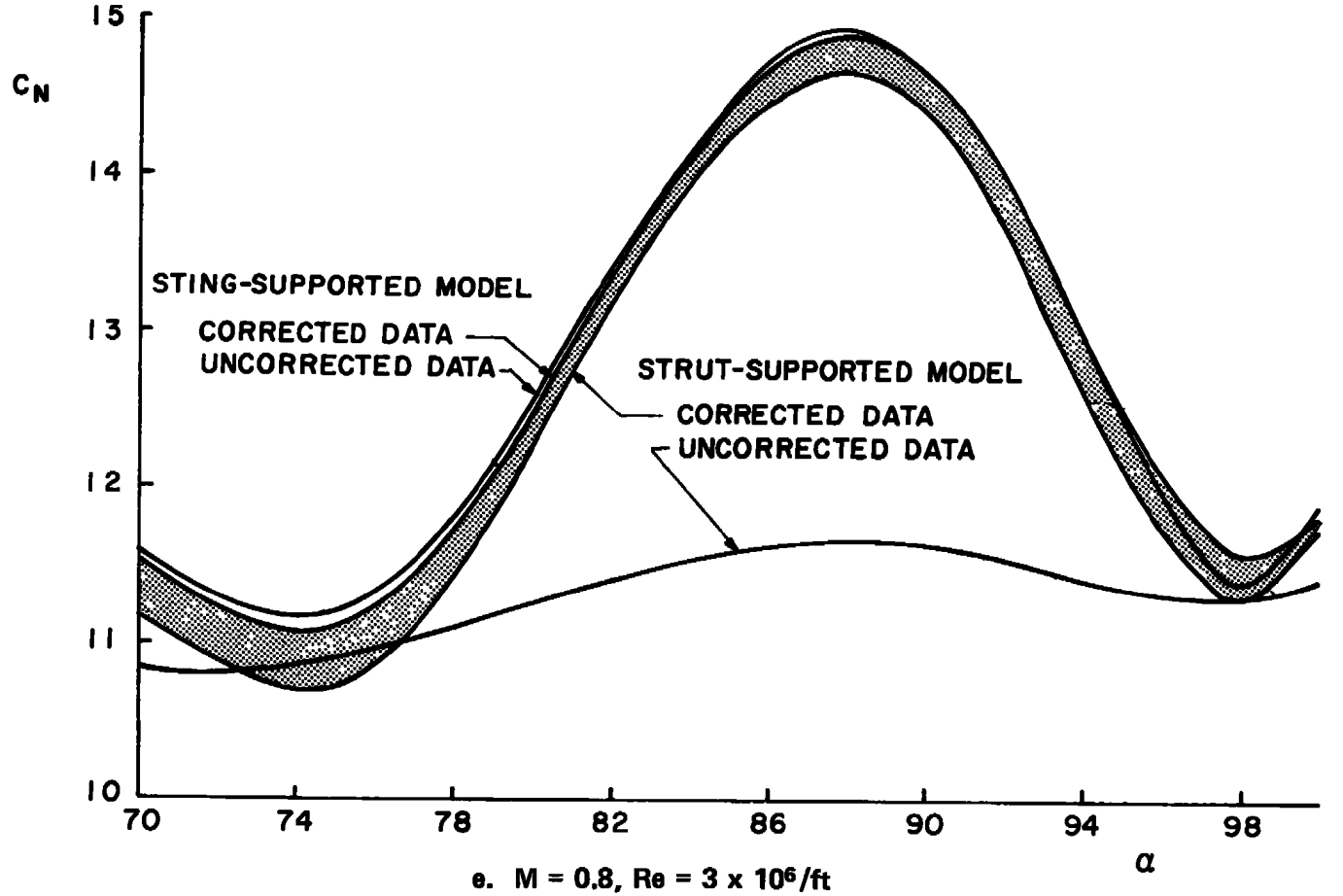

e. M = 0.8, Re = 3 x 10^6/ft
Figure 9. Continued.

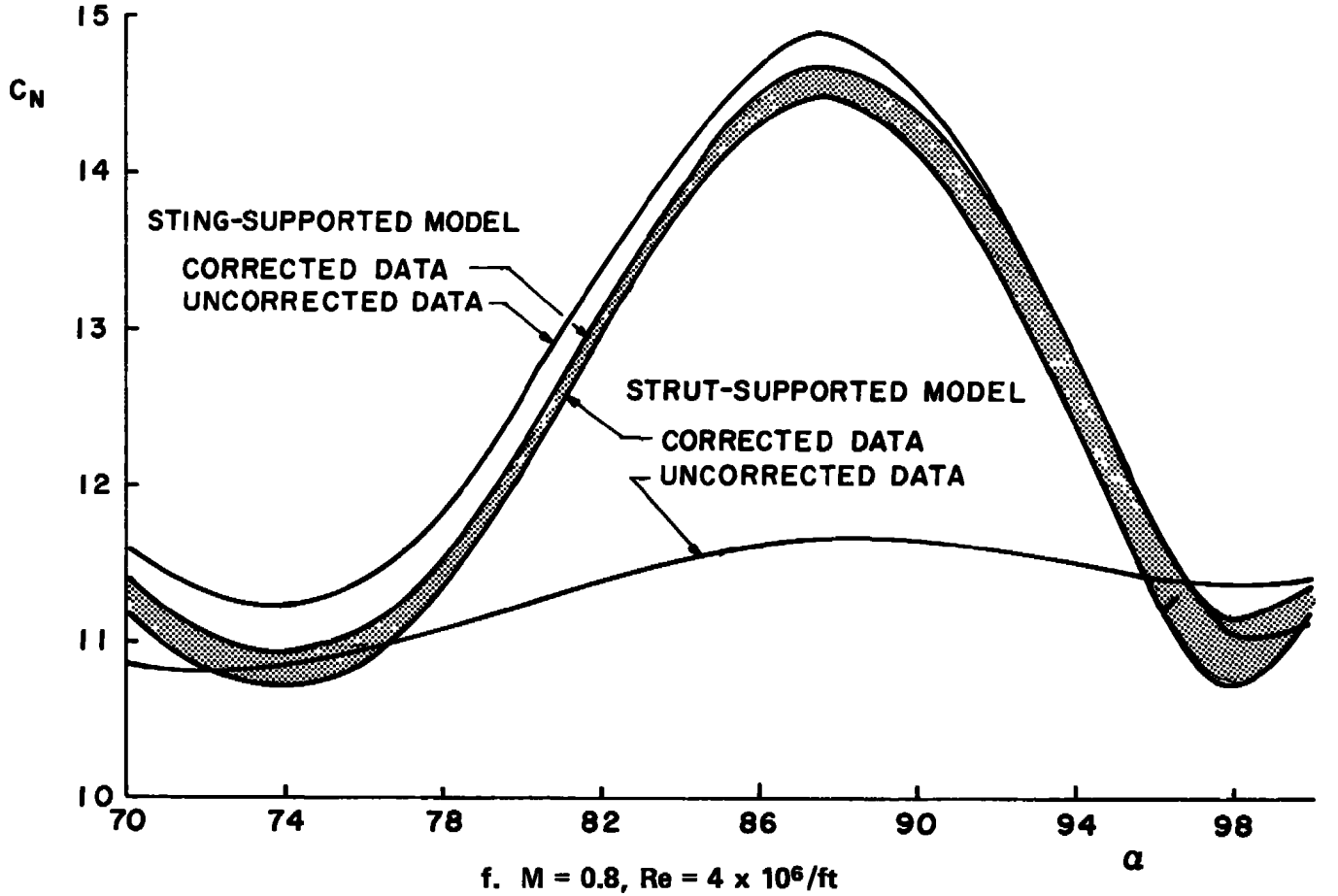

f. M = 0.8, Re = 4 x 10^6/ft

Figure 9. Continued.

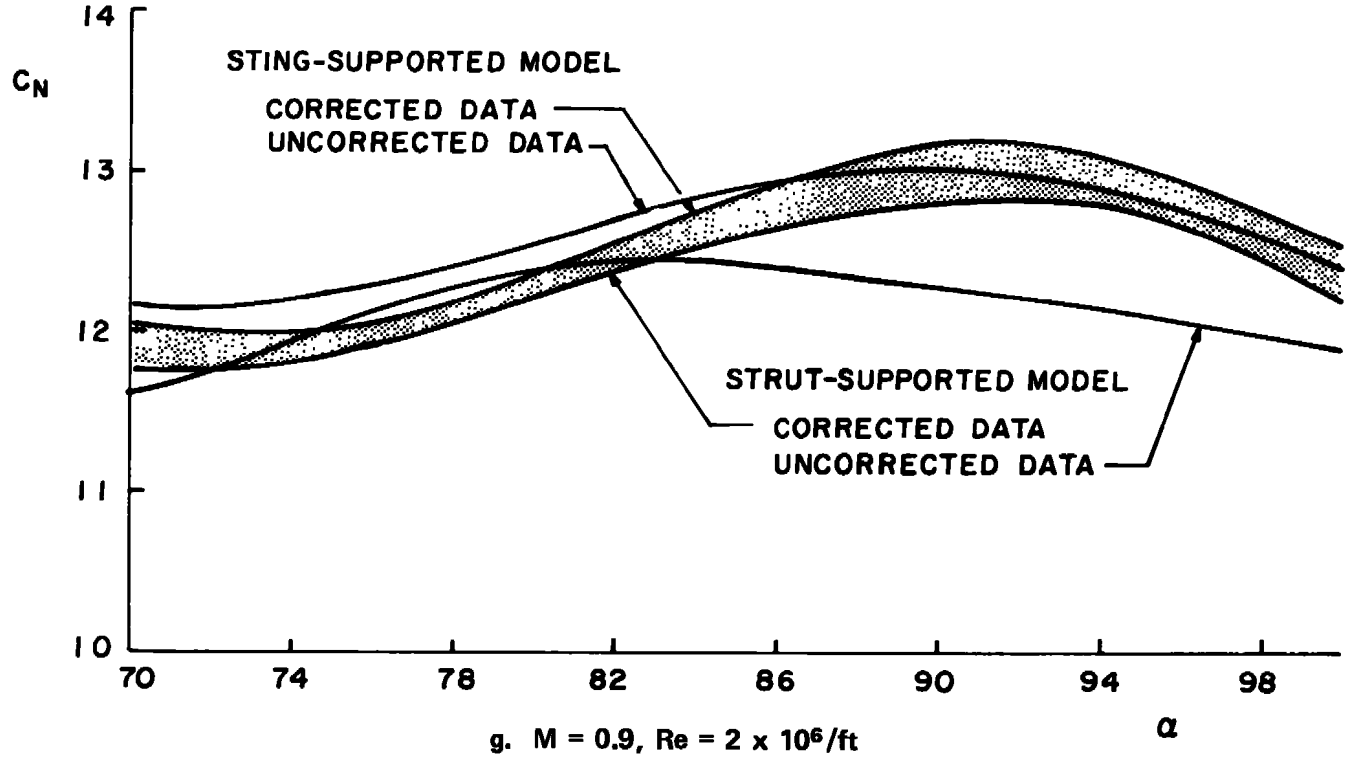

g. M = 0.9, Re = 2 x 10^6/ft

Figure 9. Continued.

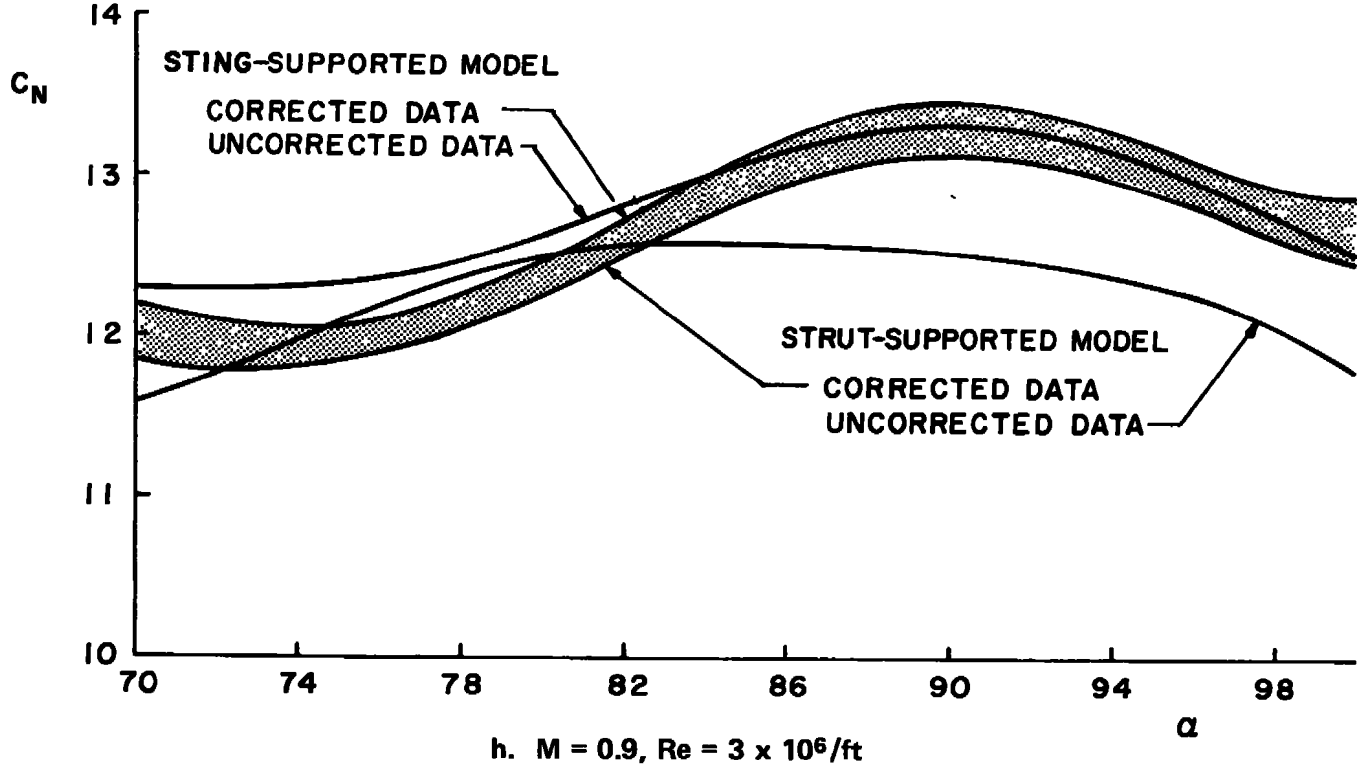

h. M = 0.9, Re = 3 x 10^6/ft
Figure 9. Continued.

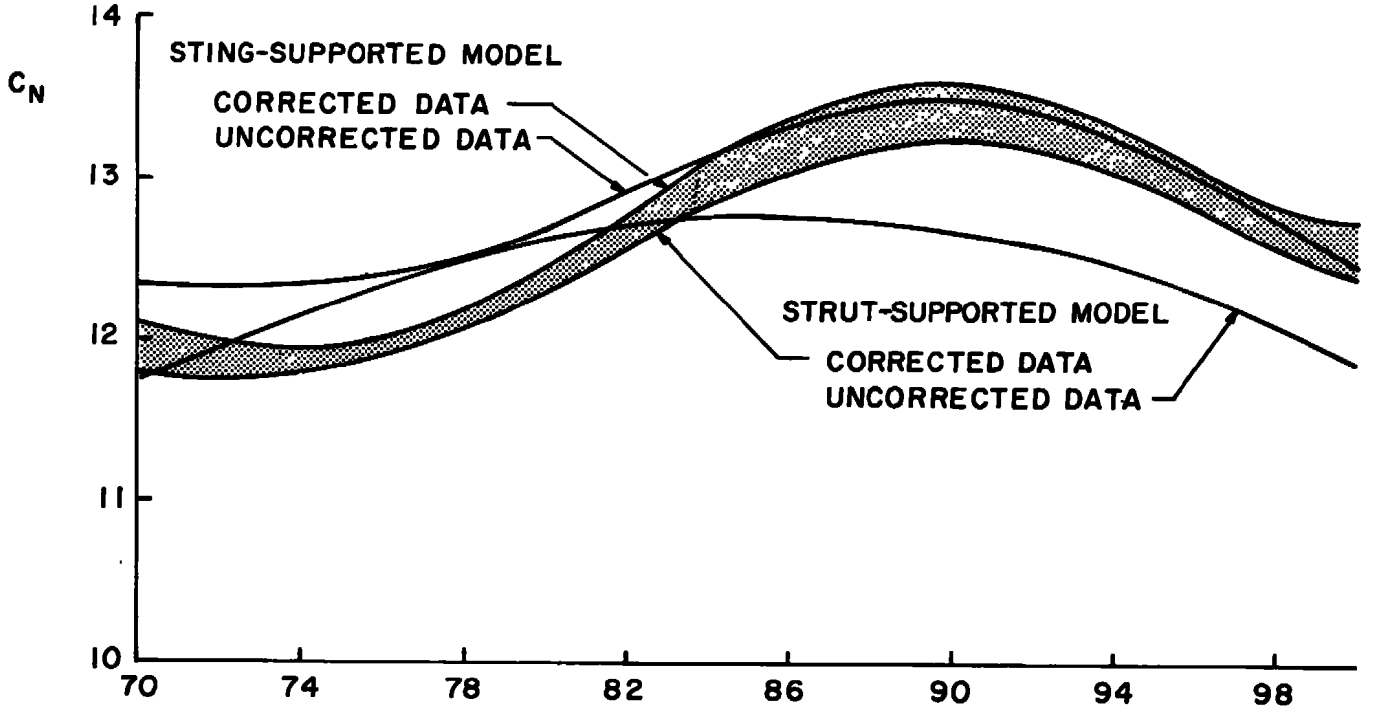

i. M = 0.9, Re = 4 x 10^6/ft

Figure 9. Concluded.

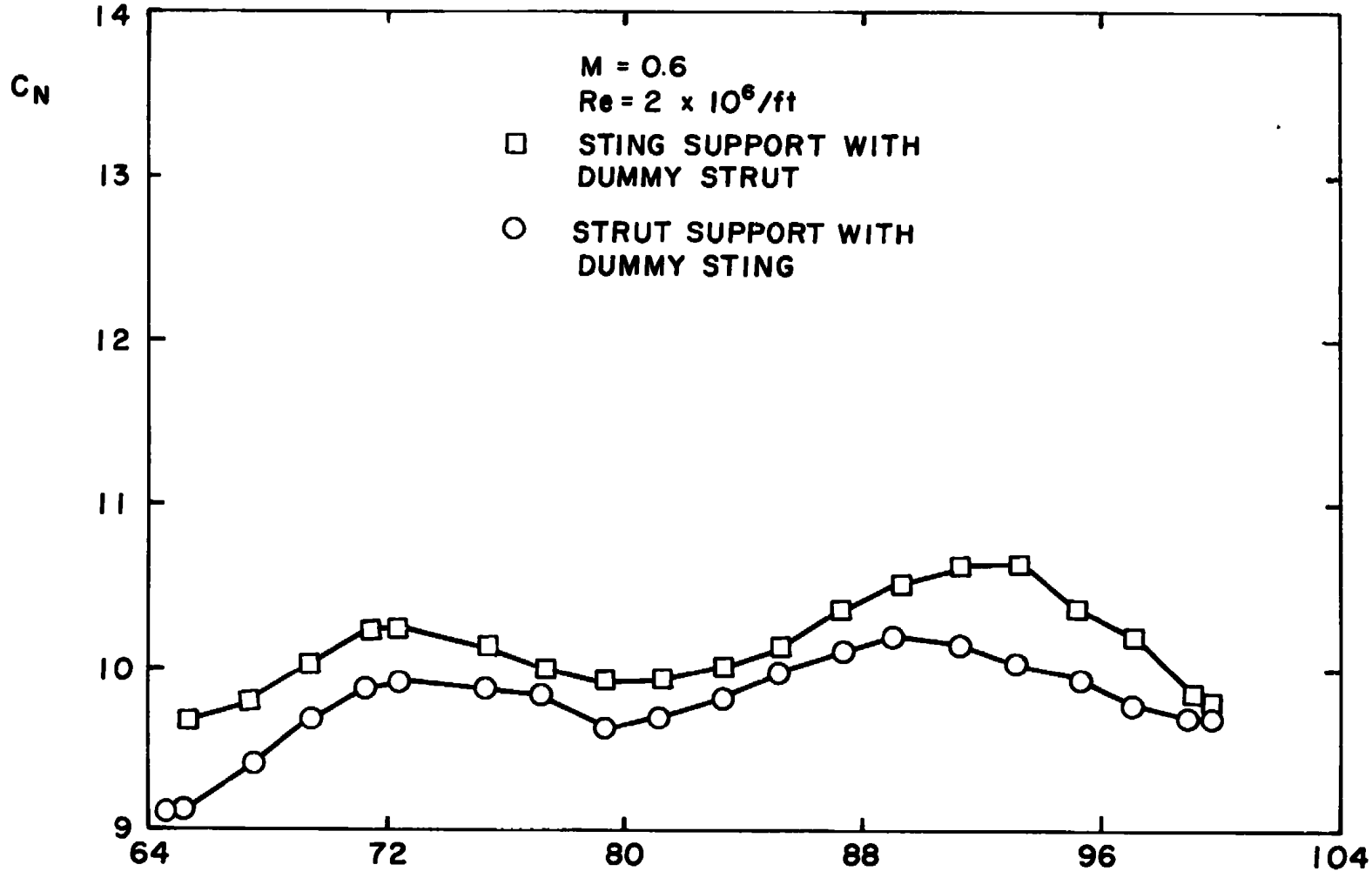

Figure 10. Sting support with dummy strut and strut support with dummy sting.

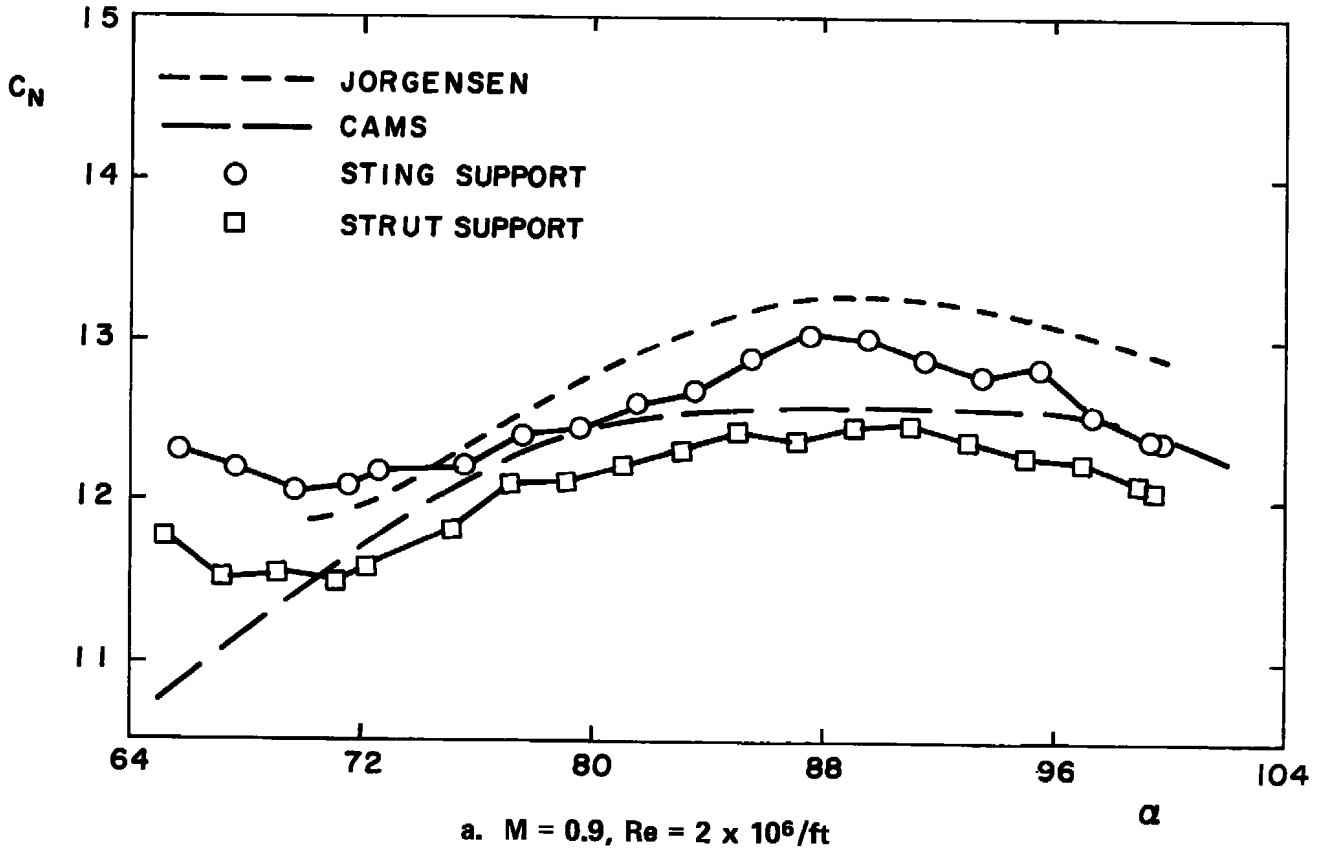

a. M = 0.9, Re = 2 x 10^6/ft

Figure 11. Analytic comparisons with sting and strut support data.

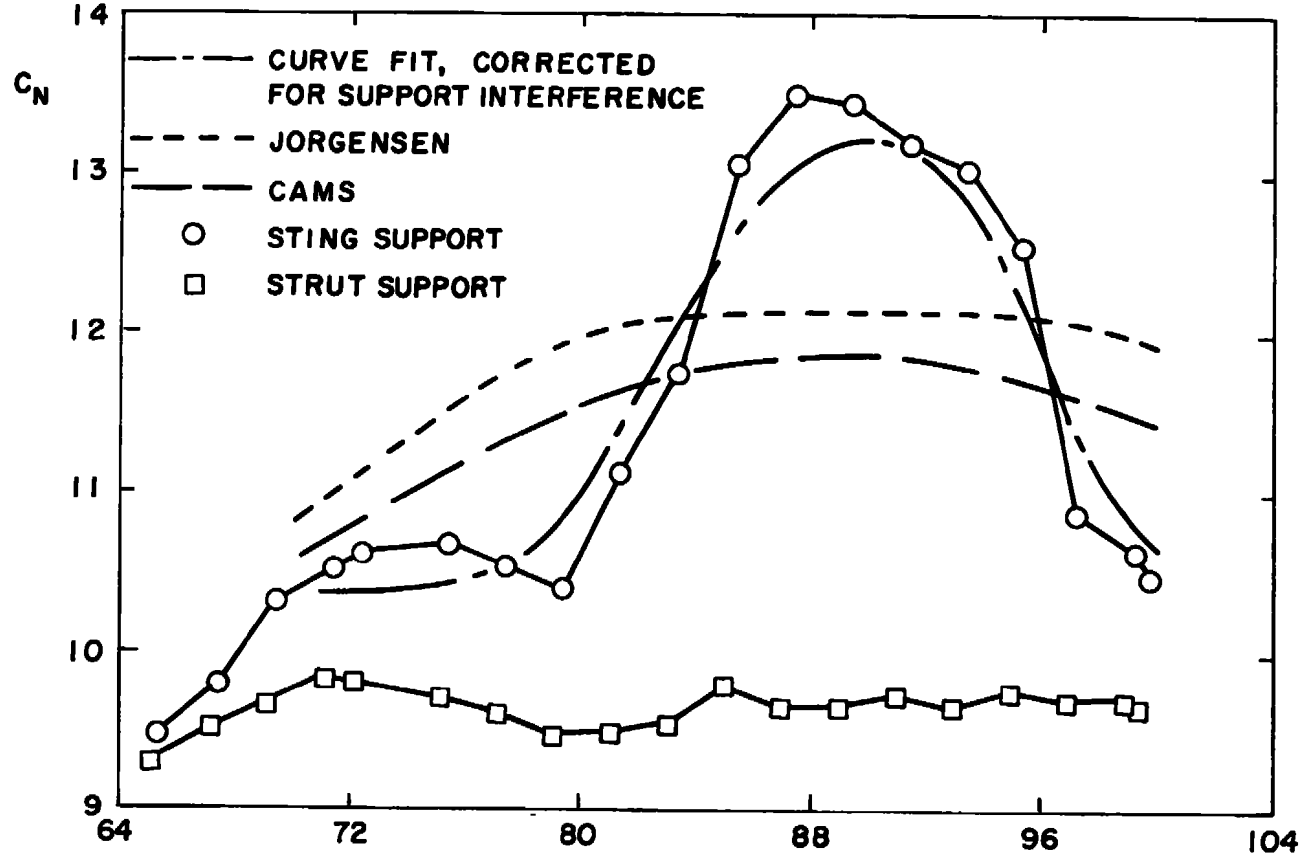

b. M = 0.6, Re = 2 x 10^6/ft

Figure 11. Continued.

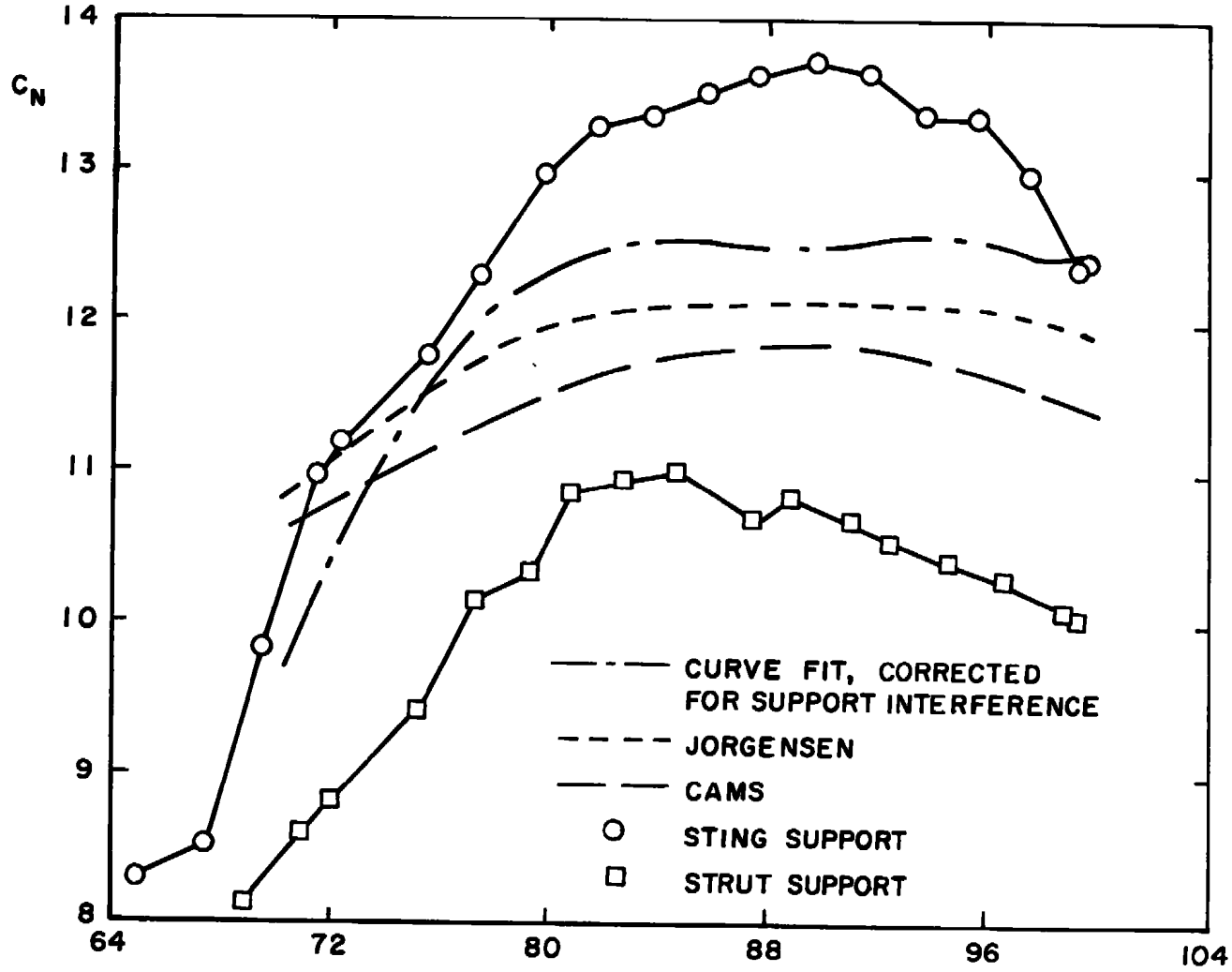

c. M = 0.6, Re = 4 x 10^6/ft

Figure 11. Concluded.

APPENDIX A
TEST DATA

The test data are presented as plots of normal-force coefficient (C_N), pitching-moment coefficient (C_m), and the distance of the center of pressure from the center of the model in model diameters (X_{CP}) versus pitch angle (α).

The plots are grouped by configuration and Mach number. Most plots show angle-of-attack surveys from 66 to 100 deg for three Reynolds numbers. The uncertainty in the measurements is less than the symbol size used.

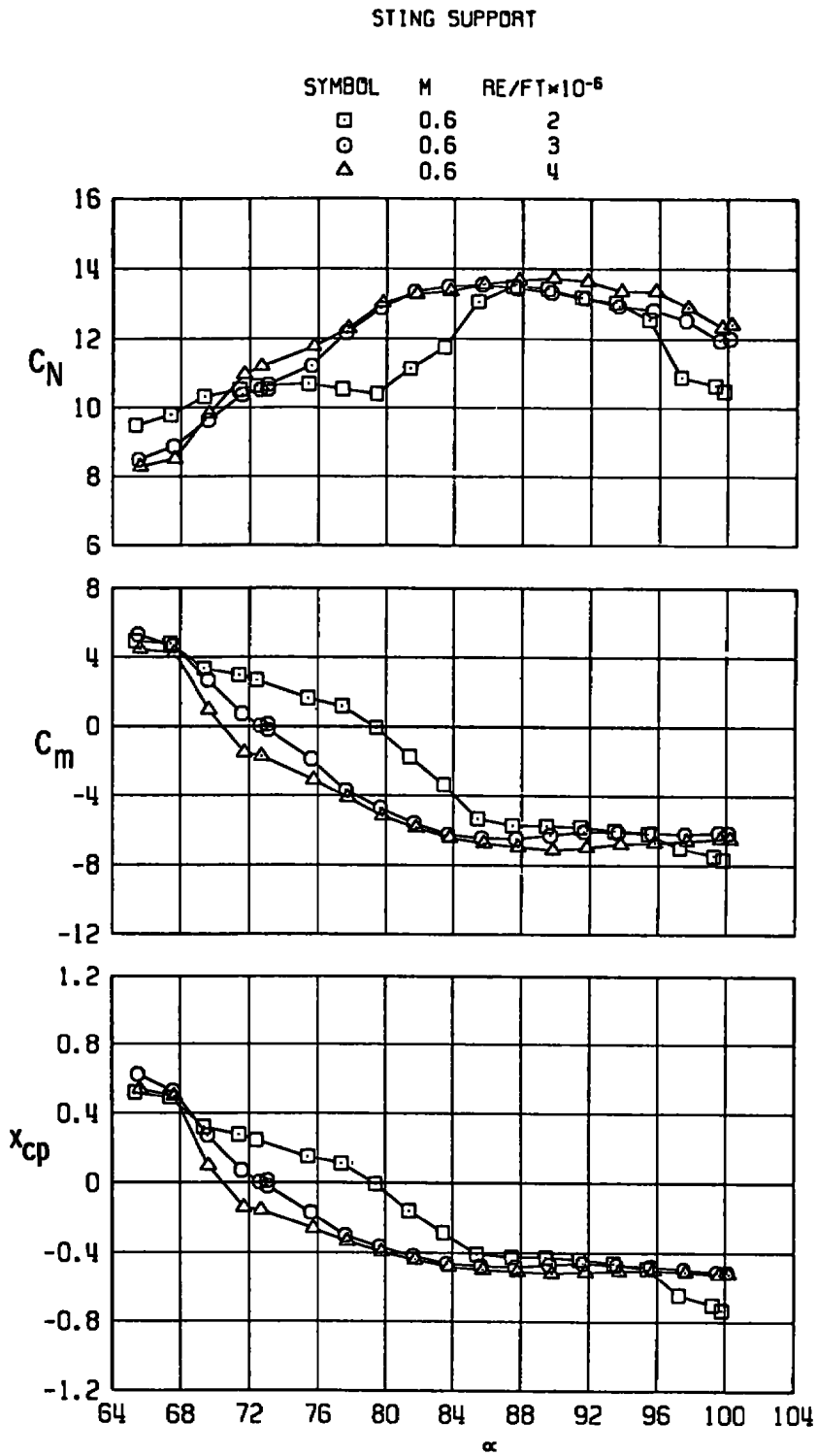

a. M = 0.6

Figure A-1. Sting support.

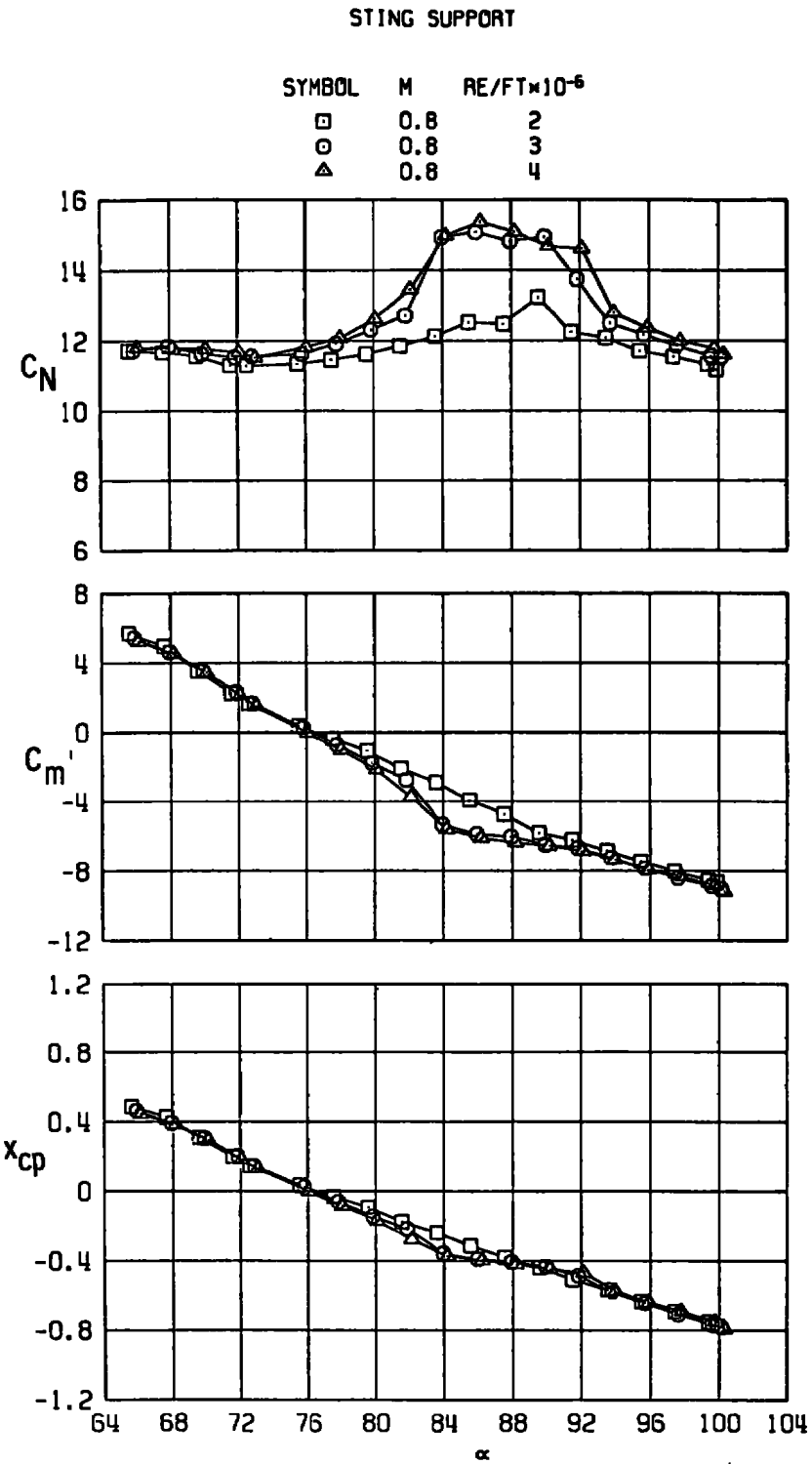

b. M = 0.8

Figure A-1. Continued.

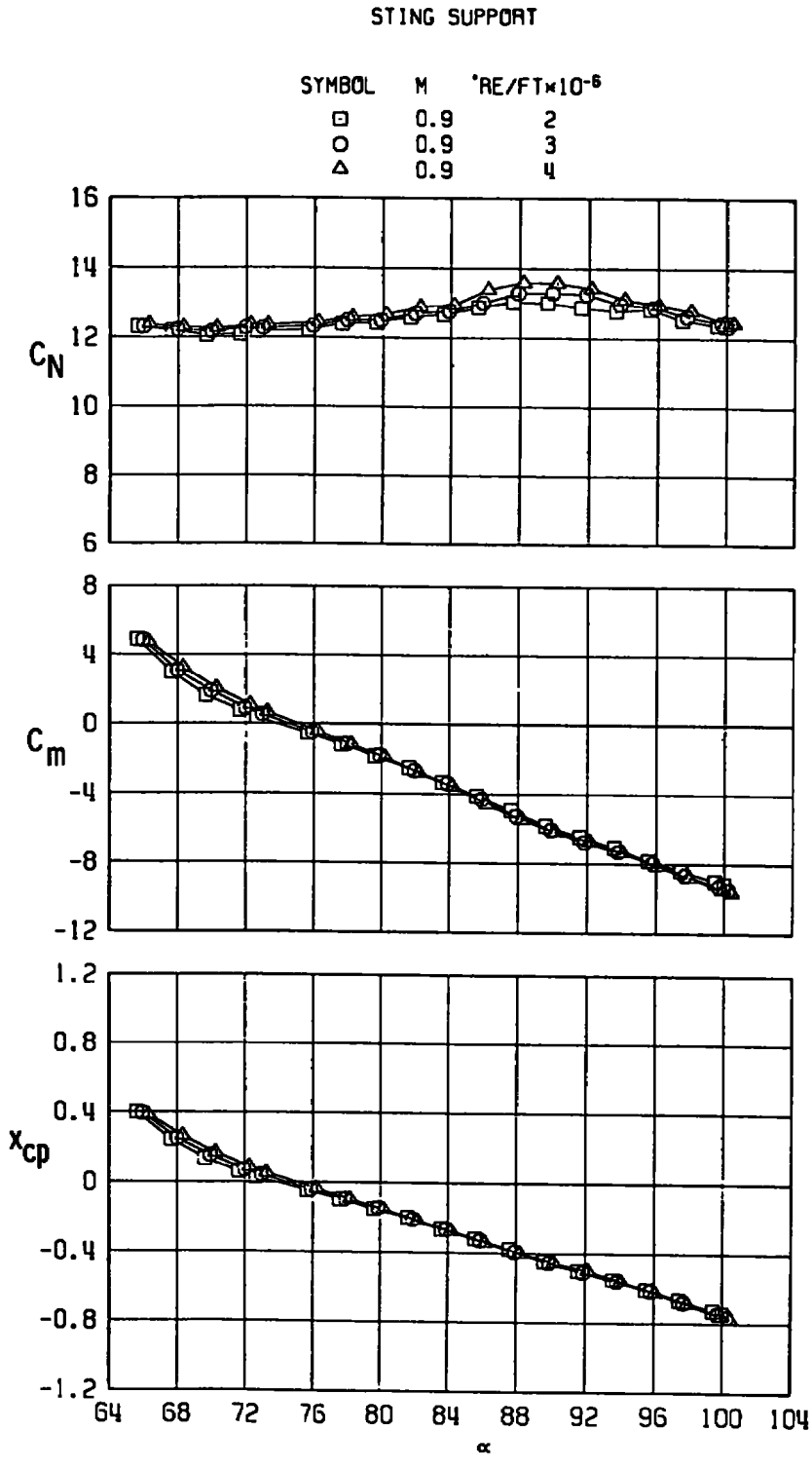

c. M = 0.9
Figure A-1. Concluded.

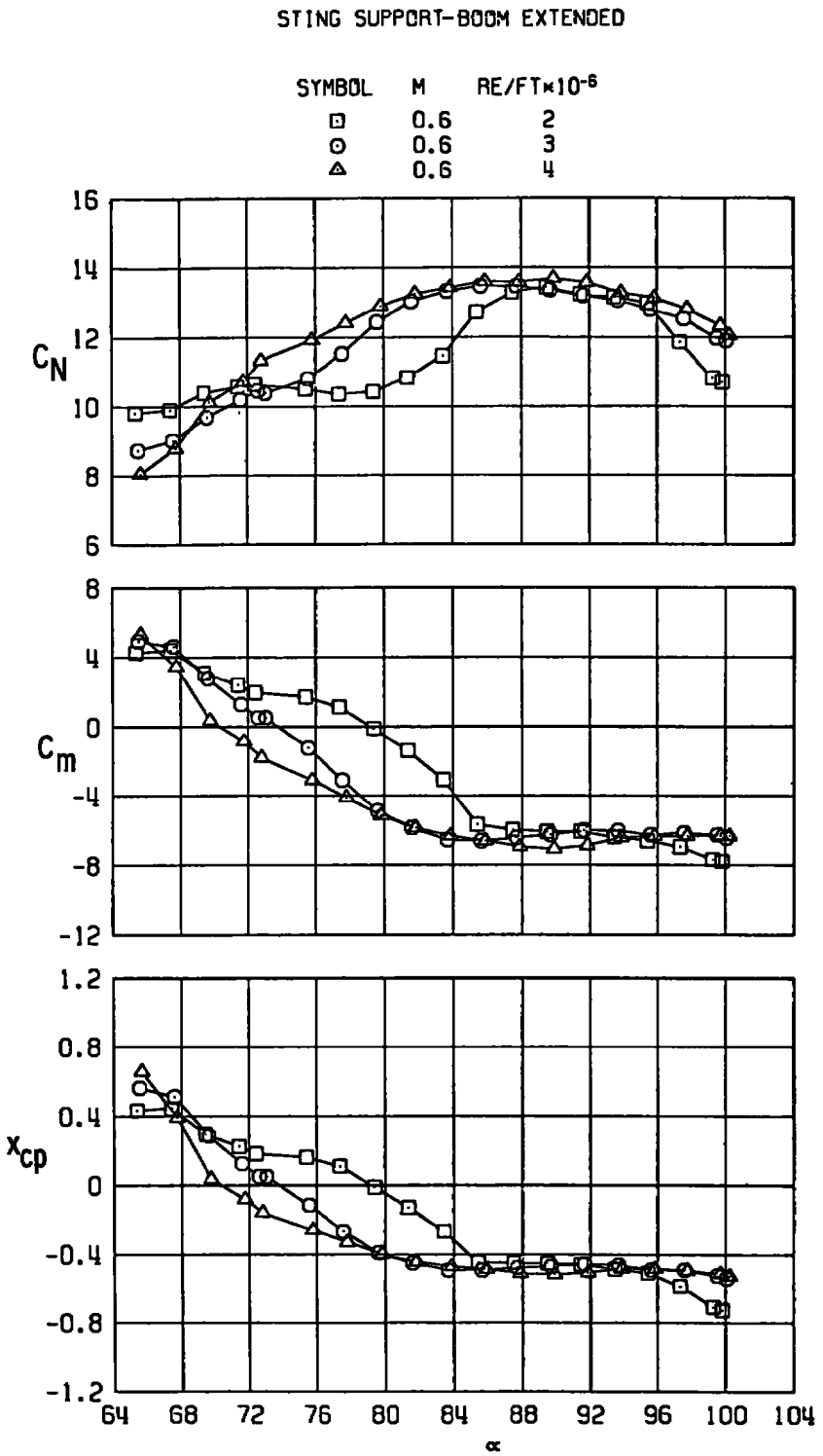

a. M = 0.6

Figure A-2. Sting support — boom extended.

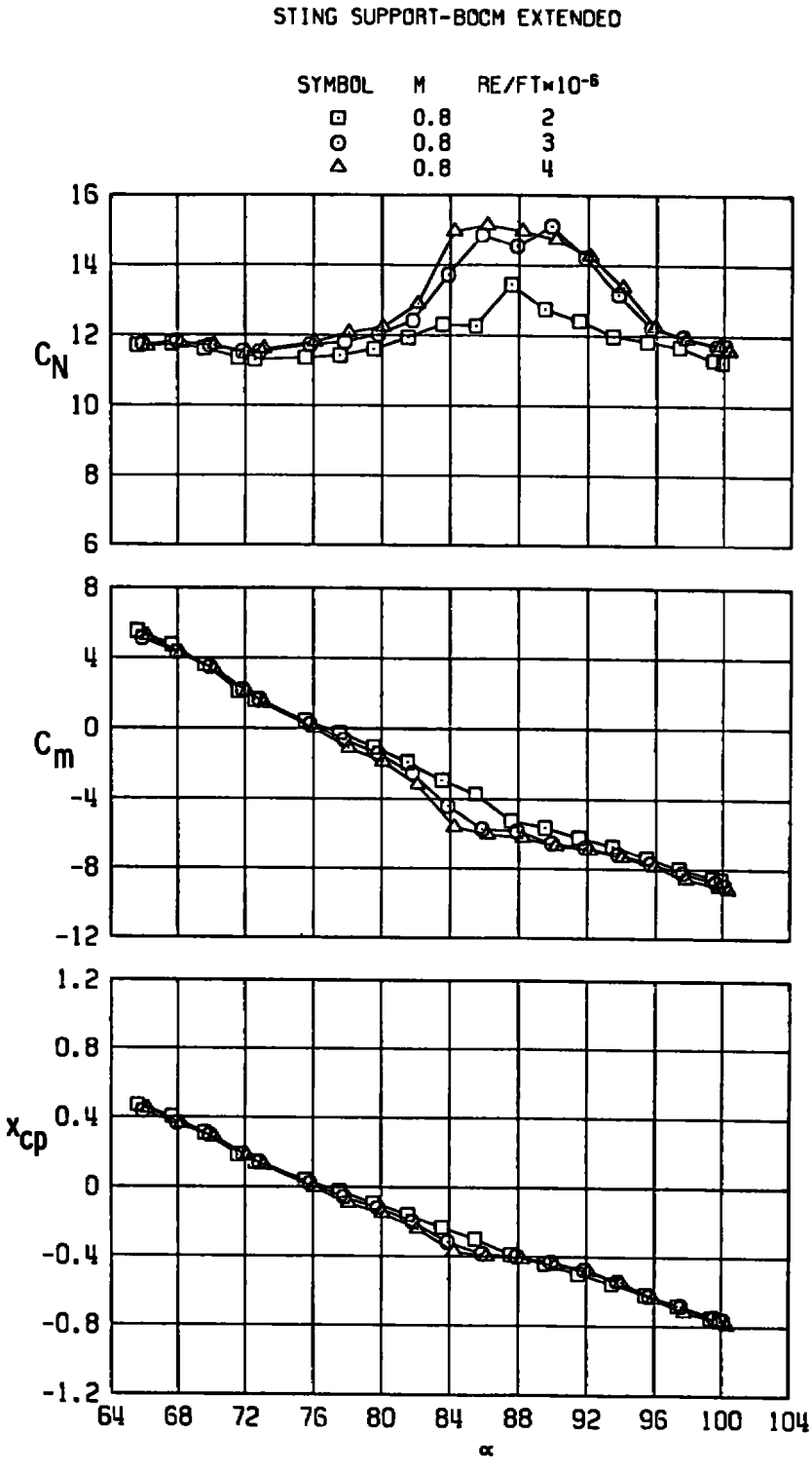

b. M = 0.8

Figure A-2. Continued.

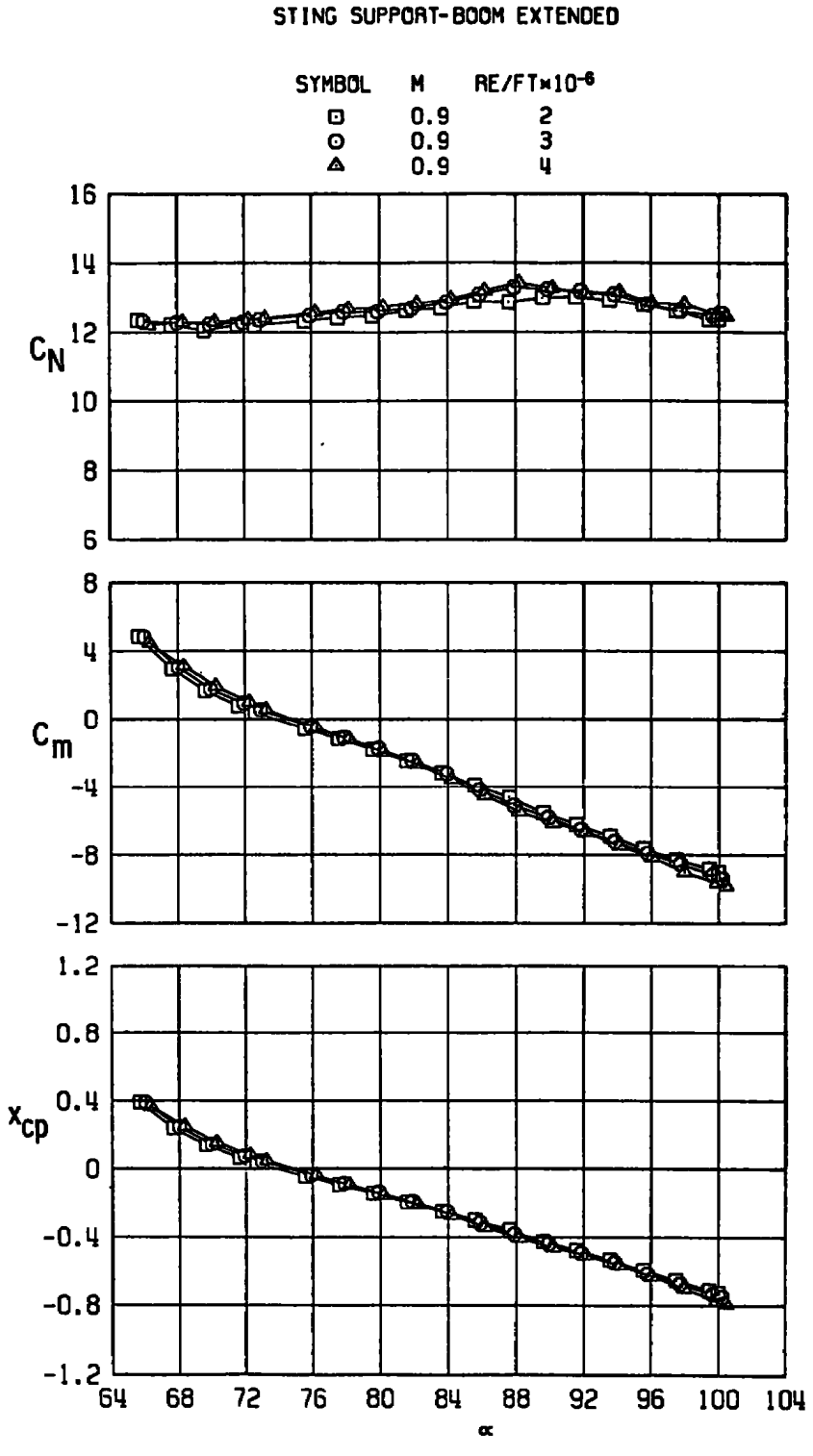

c. M = 0.9

Figure A-2. Concluded.

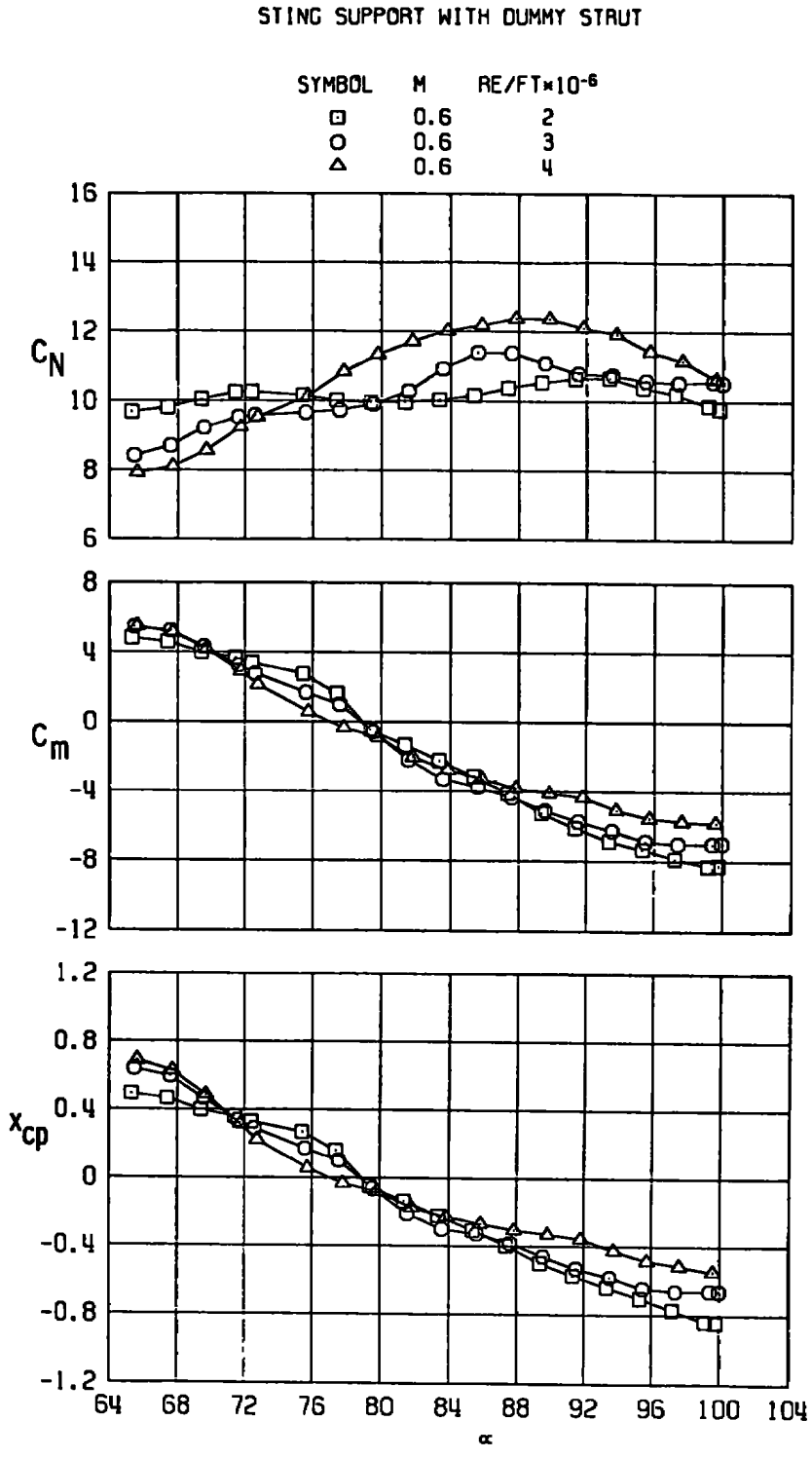

a. M = 0.6

Figure A-3. Sting support with dummy strut.

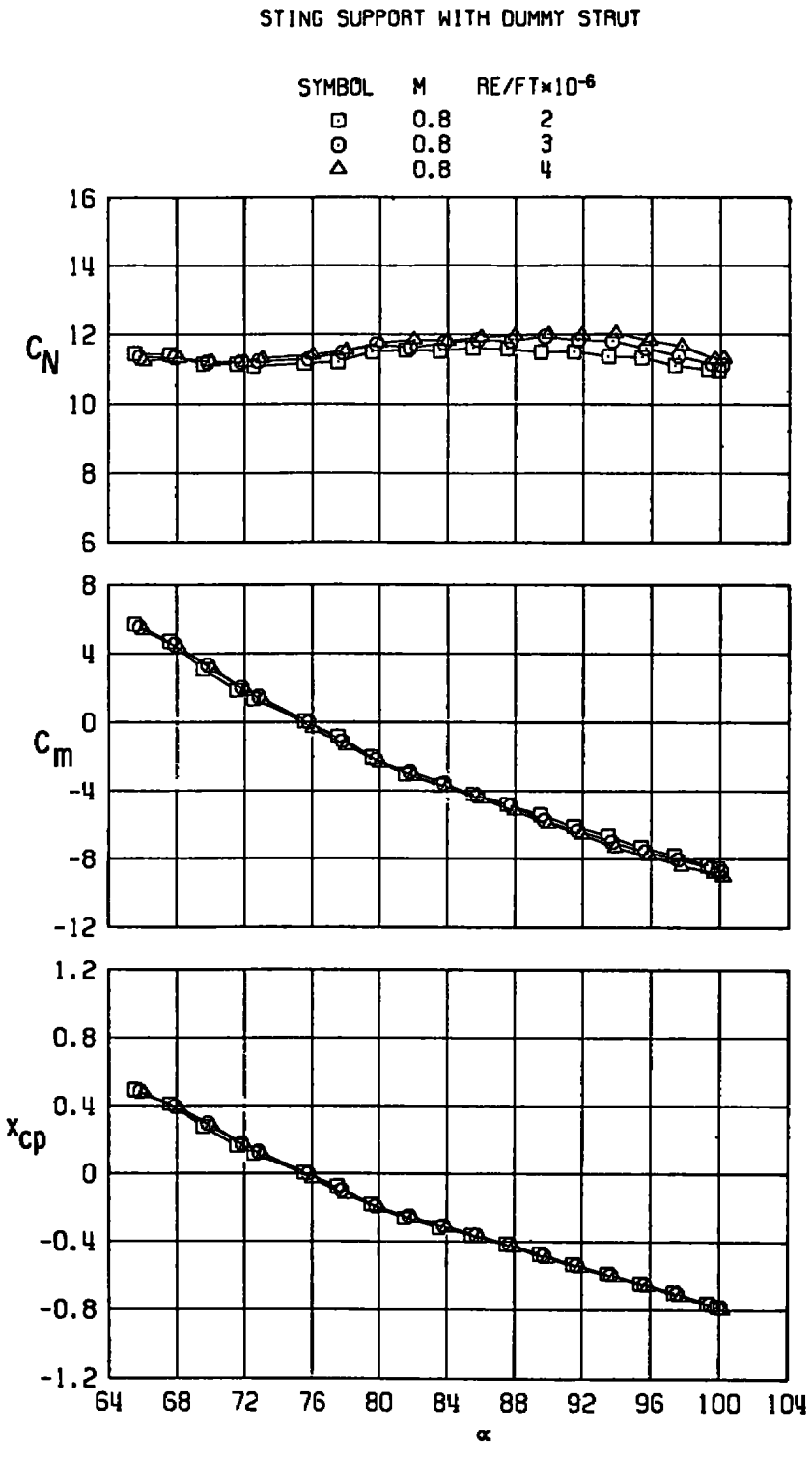

b. M = 0.8

Figure A-3. Continued.

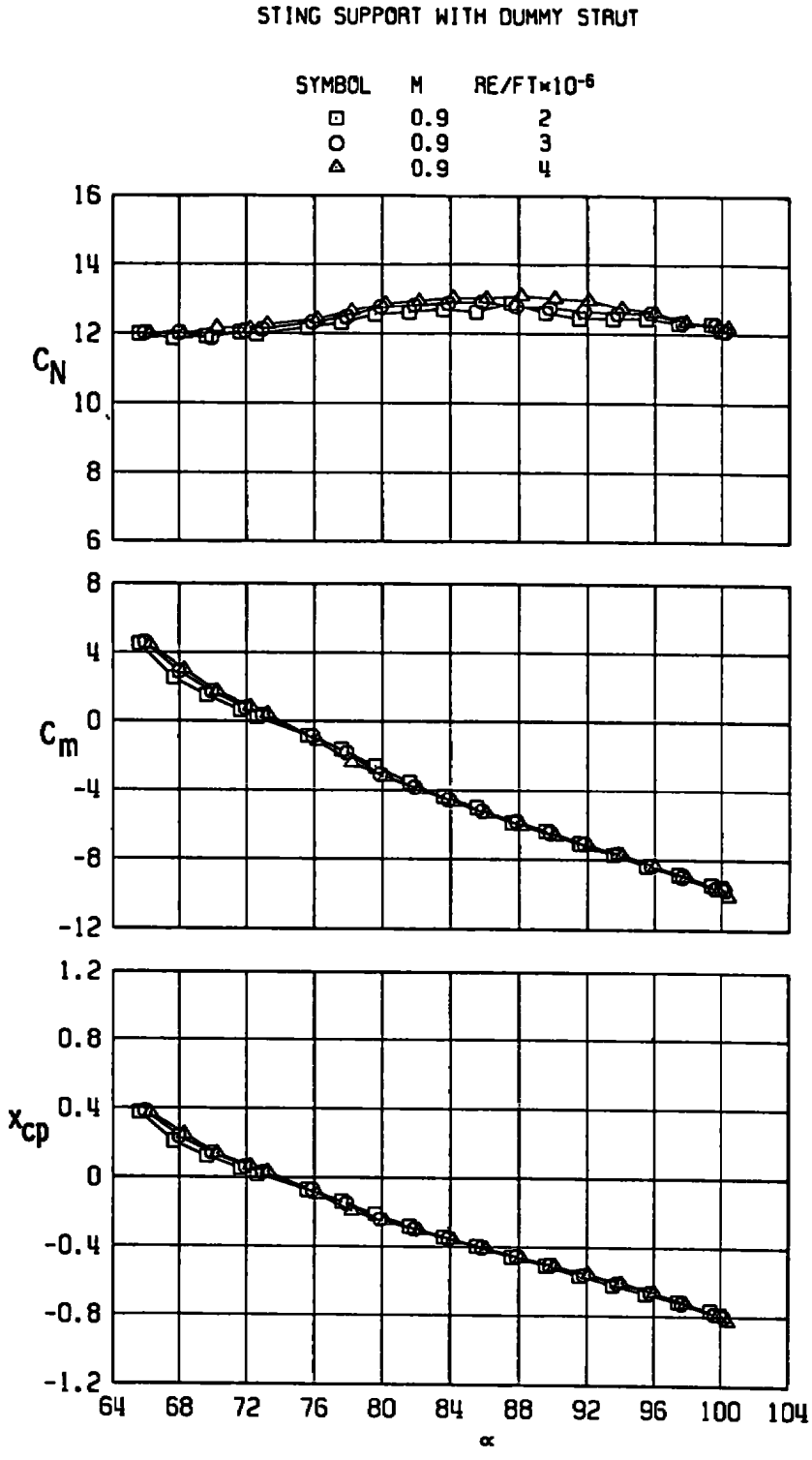

c. M = 0.9

Figure A-3. Concluded.

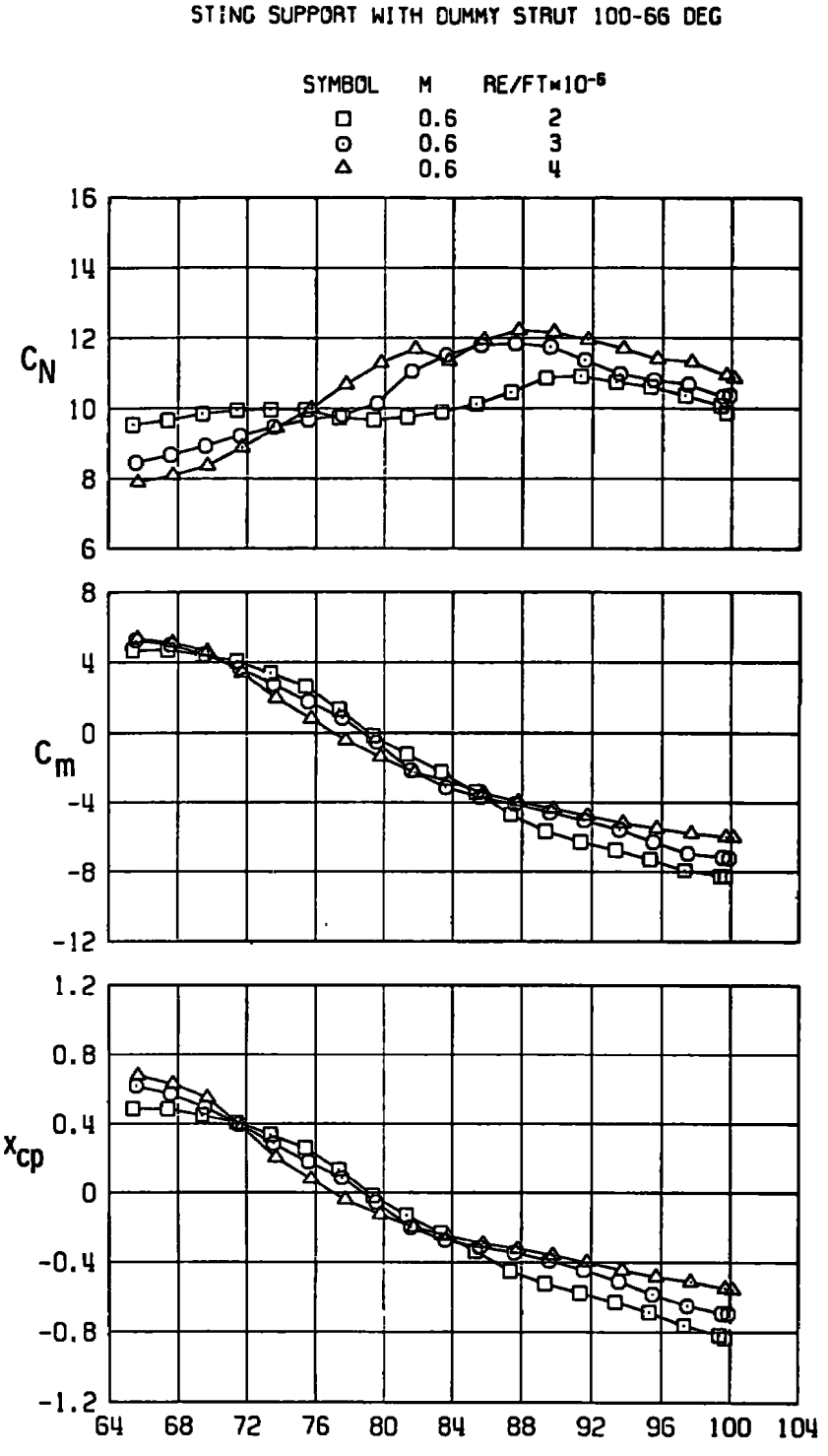

a. M = 0.6

Figure A-4. Sting support with dummy strut, 100 to 66 deg.

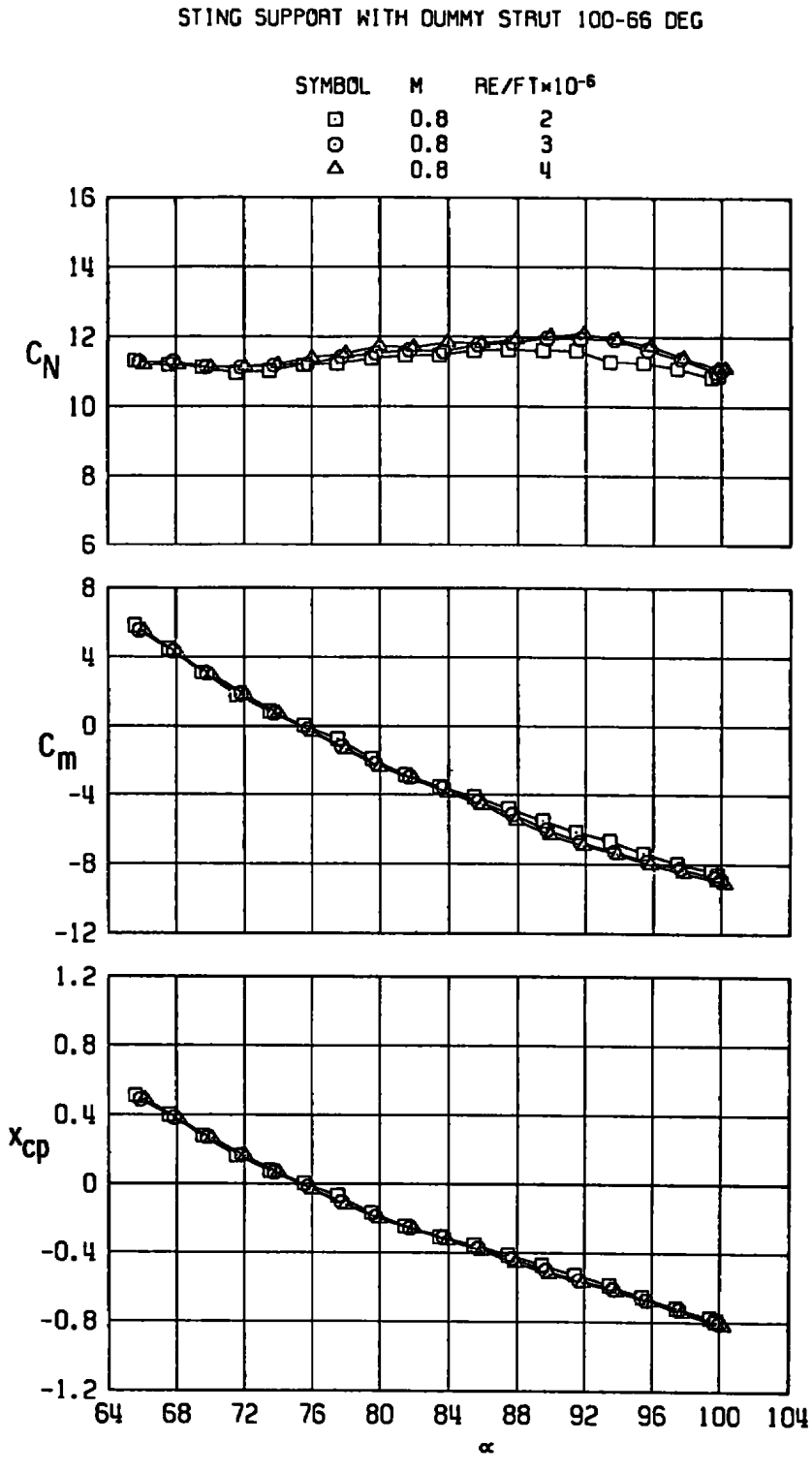

b. M = 0.8

Figure A-4. Continued.

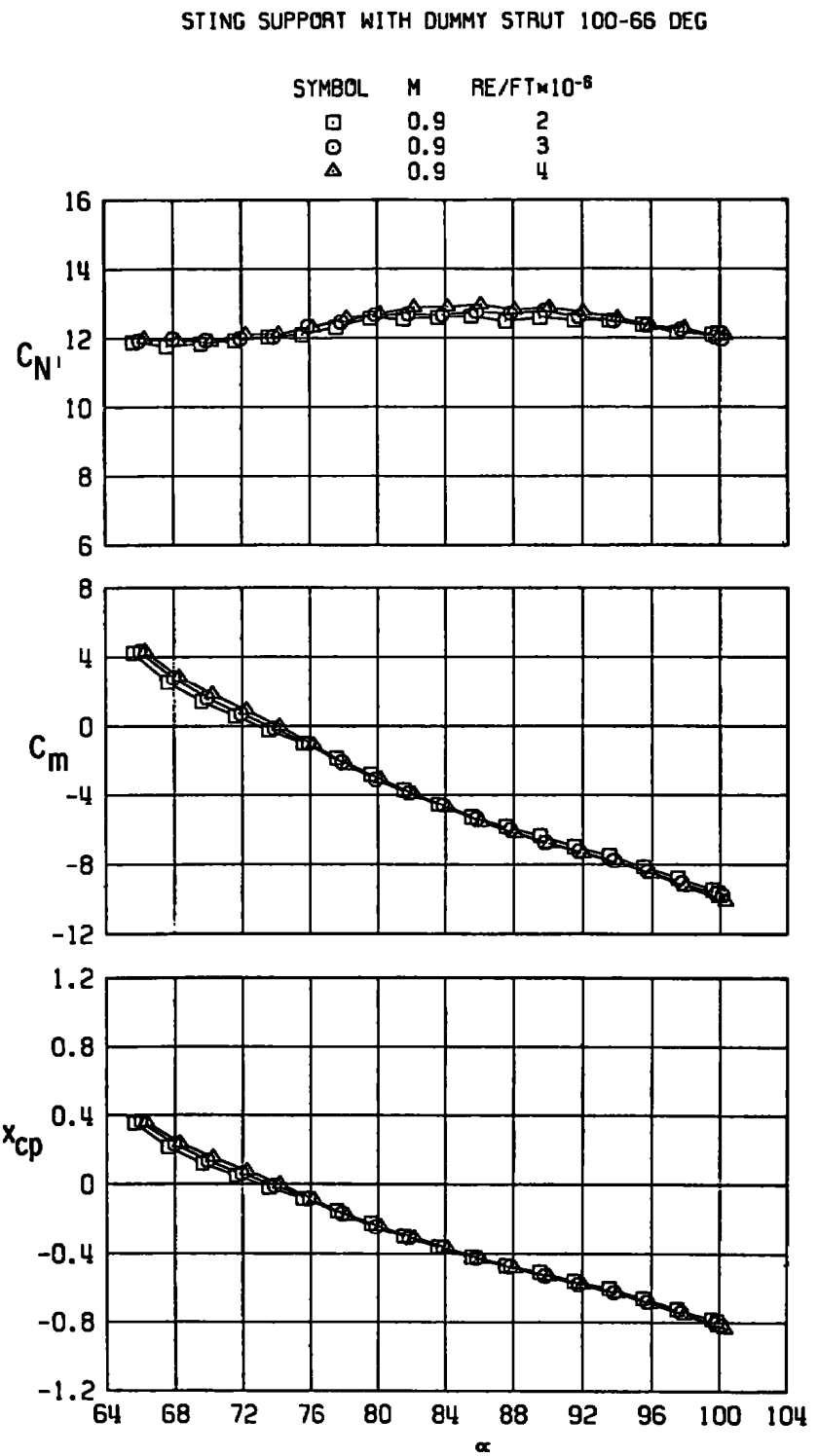

c. M = 0.9

Figure A-4. Concluded.

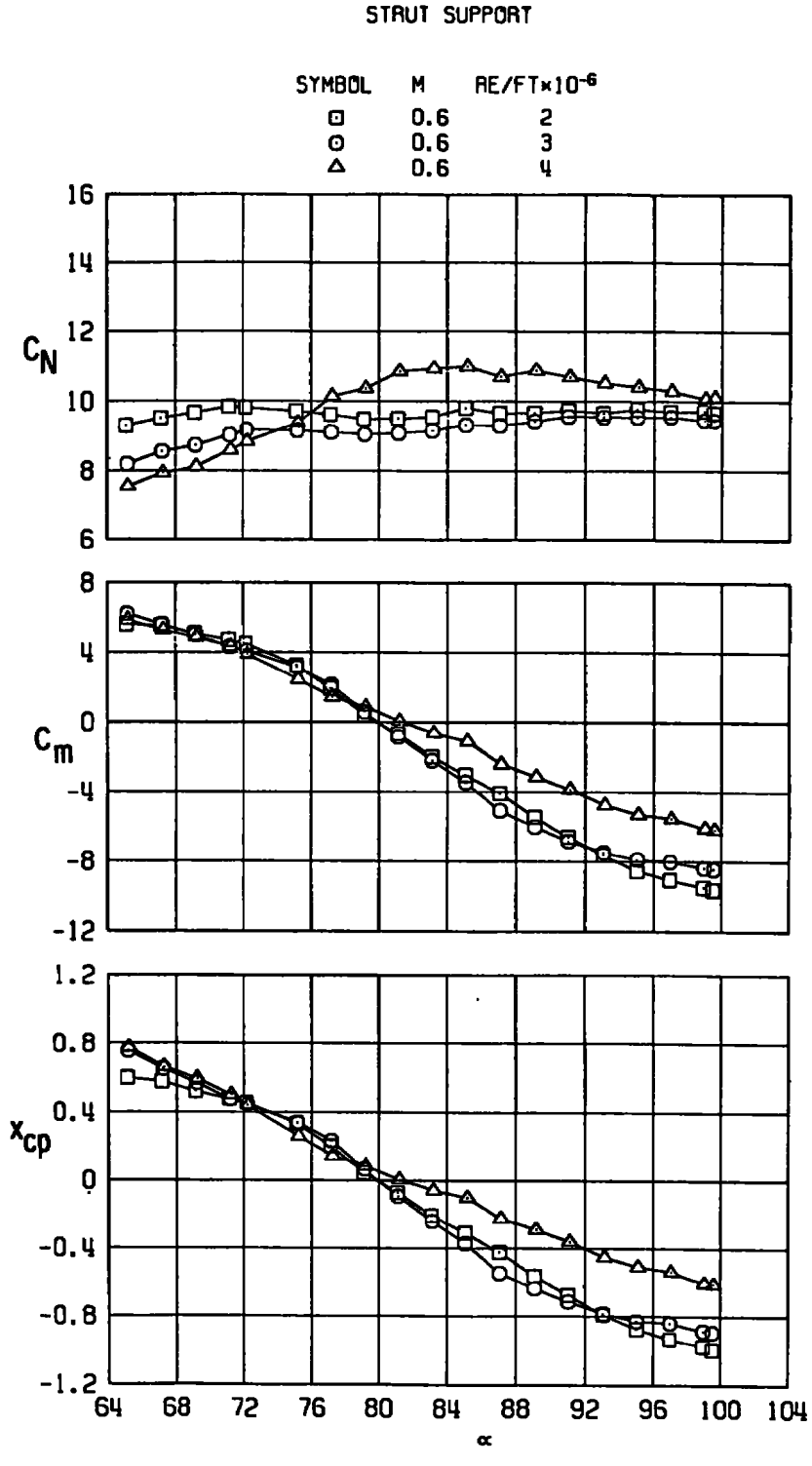

a. M = 0.6

Figure A-5. Strut support.

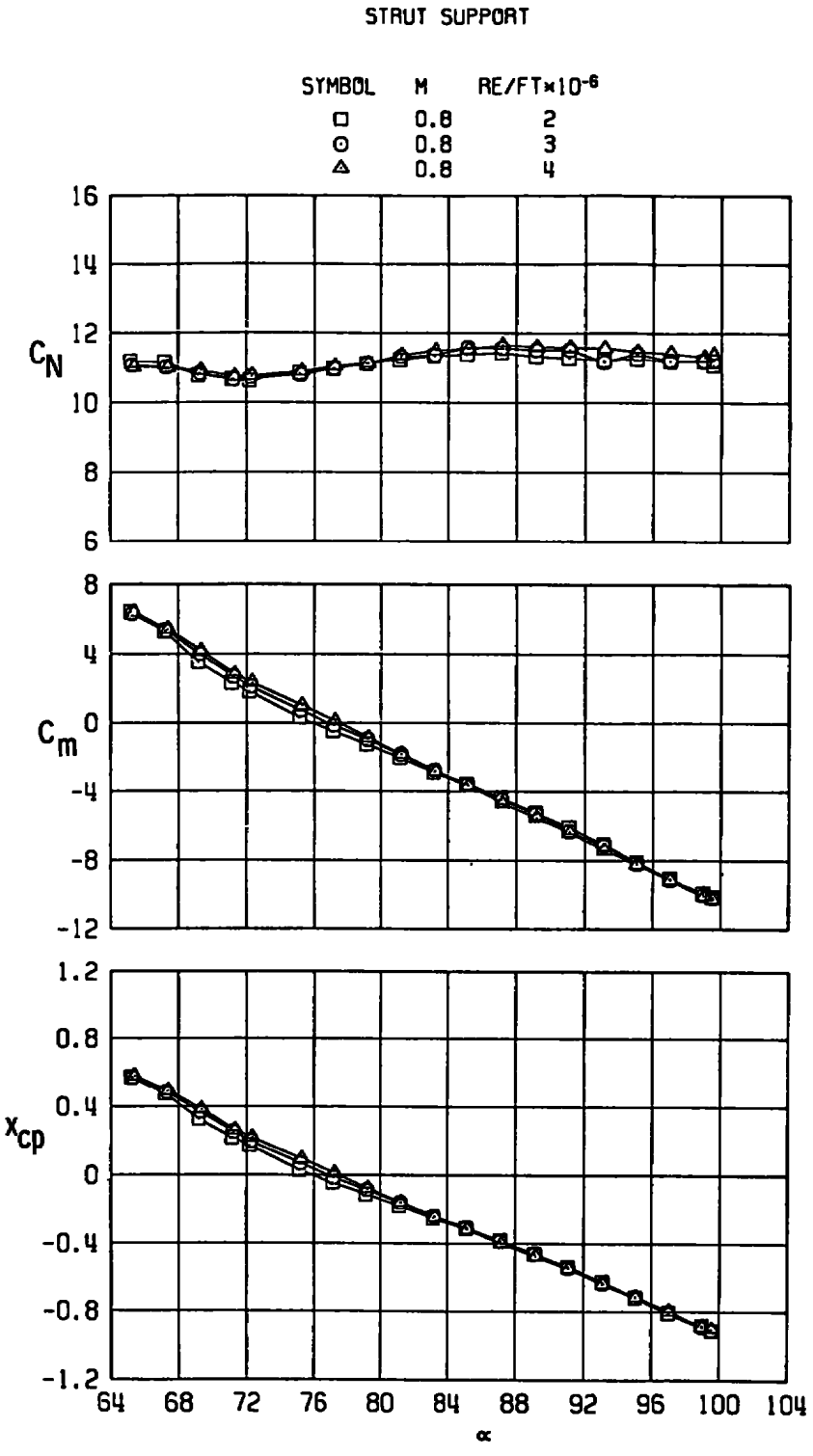

b. M = 0.8

Figure A-5. Continued.

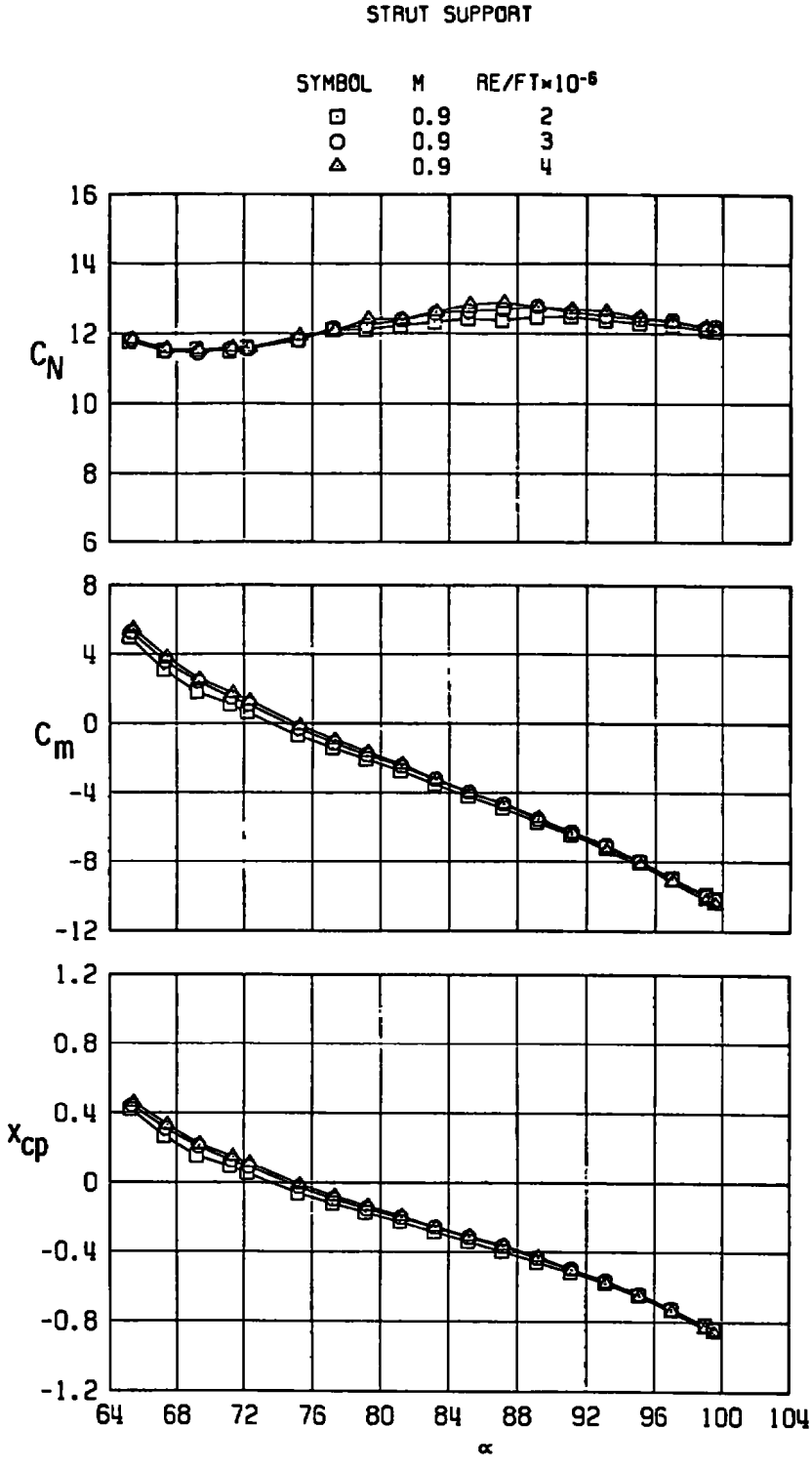

c. M = 0.9

Figure A-5. Concluded.

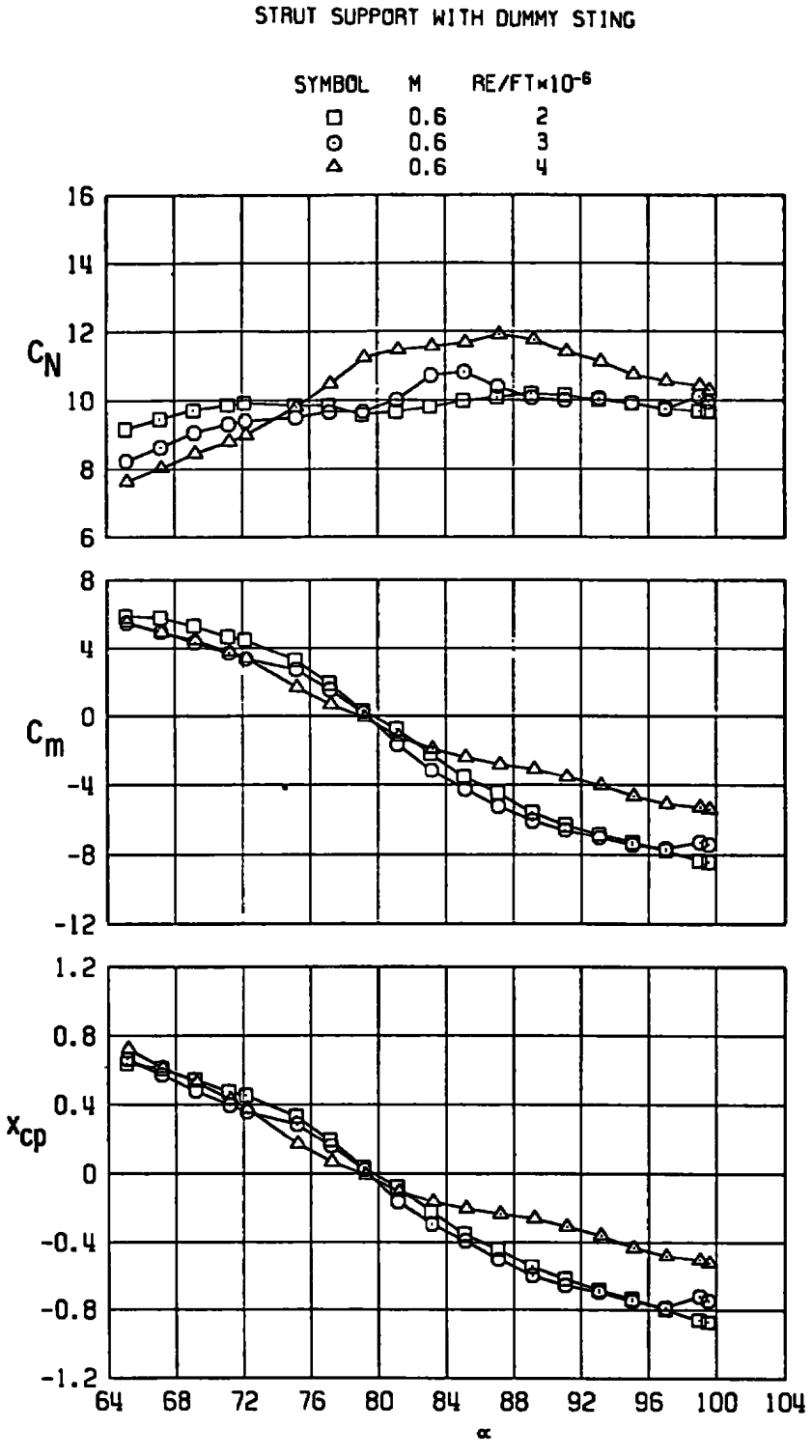

a. M = 0.6

Figure A-6. Strut support with dummy sting.

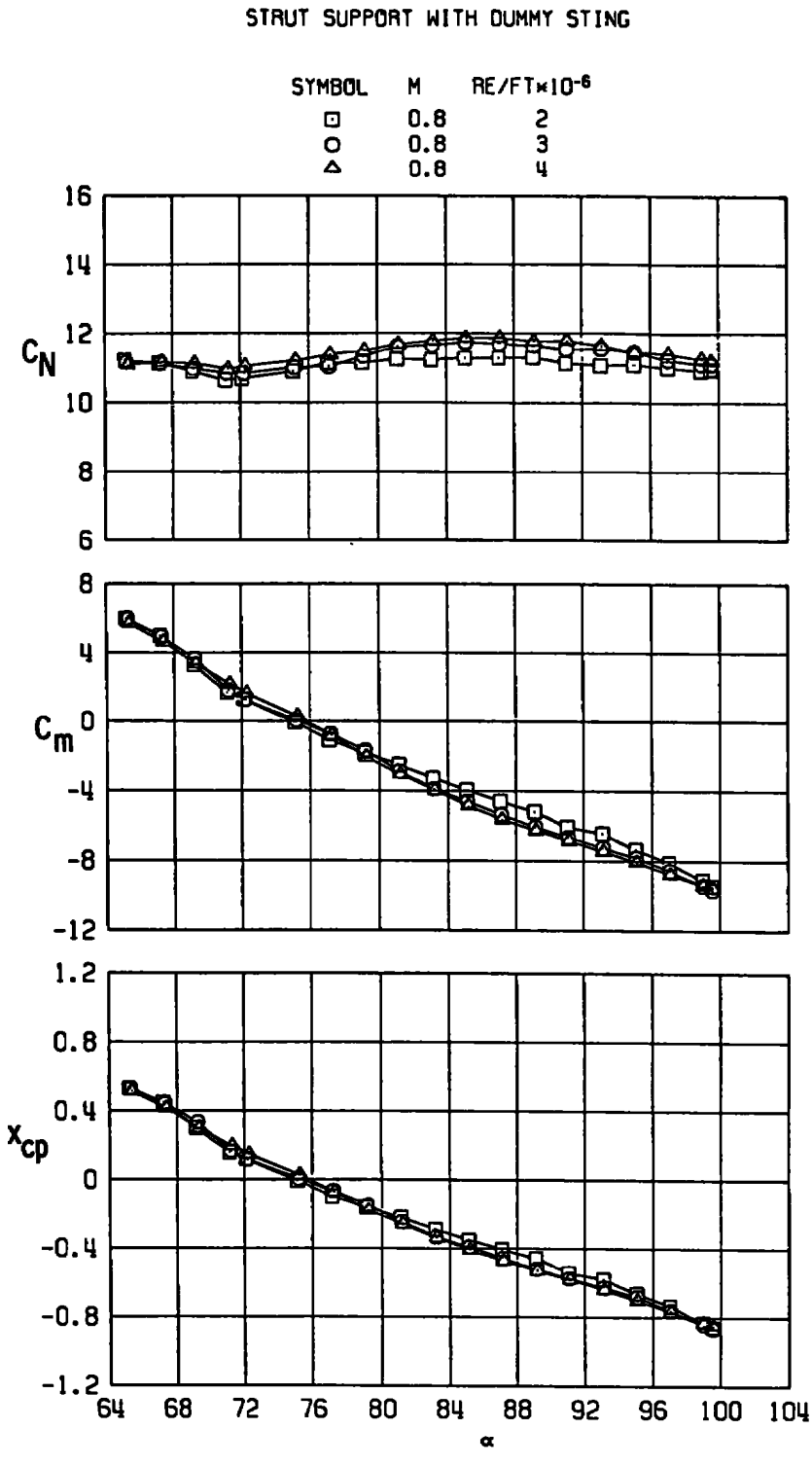

b. M = 0.8

Figure A-6. Continued.

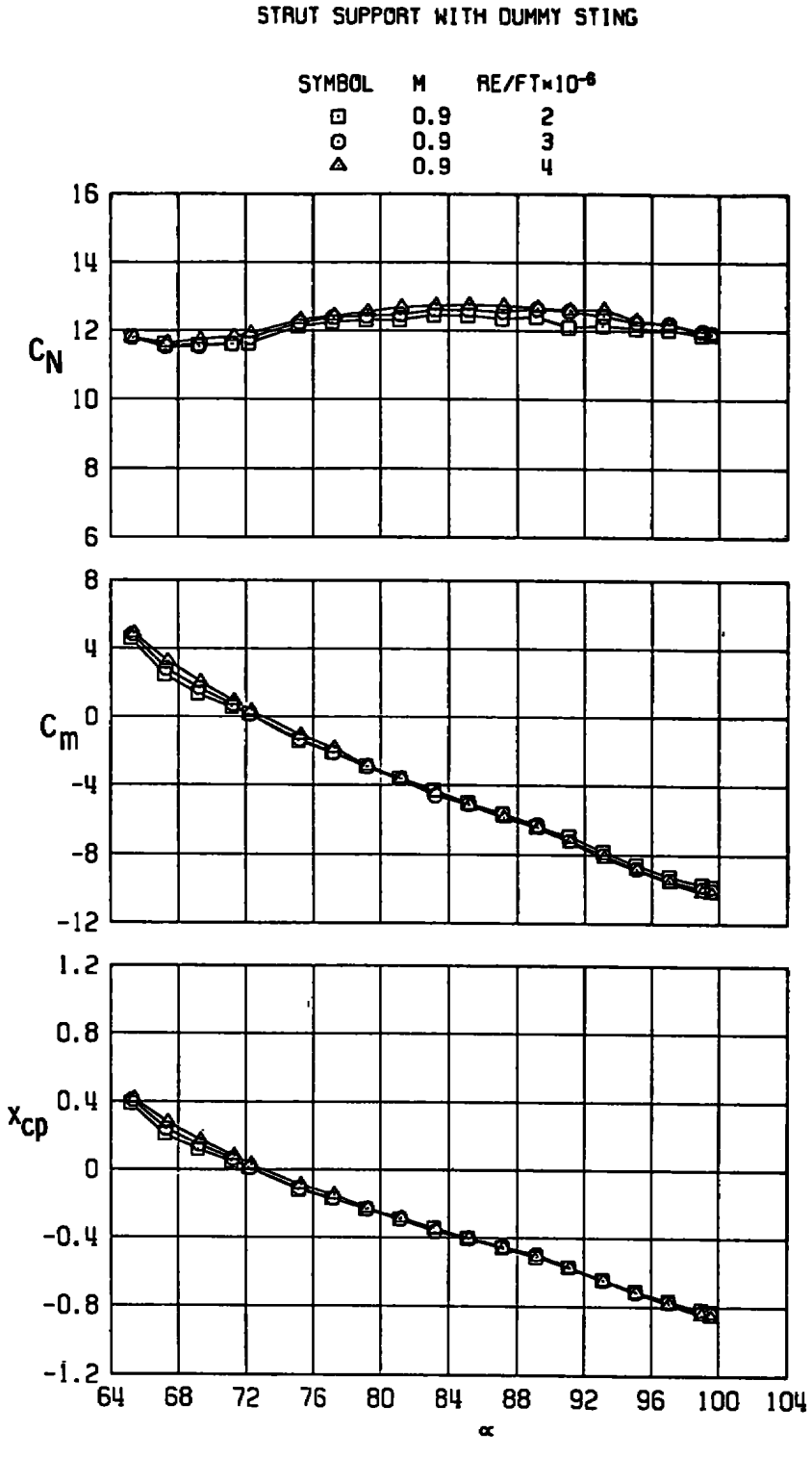

c. M = 0.9

Figure A-6. Concluded.

APPENDIX B
WALL INTERFERENCE STUDY BY VORTEX LATTICE

An analytic study was conducted to estimate wall interference. A vortex lattice representation was developed for the model and tunnel using the techniques of Ref. 8. The vortex-lattice model of the ogive cylinder is presented in Fig. B-1. Vorticity was trailed from the model to provide lift, and the vortex lattice solution was used to calculate pressures for the upper and lower surfaces of the model.

Solutions were obtained for the model with and without tunnel walls and at varying distances from the wall. Local interference is defined as the difference between free-air solutions and solutions with the walls present.

$$\Delta C_P = C_{P\ (tunnel)} - C_{P\ (free\ air)}$$

Figure B-2 shows the interference obtained from these calculations with the model nose 6 in. from the wall, which is the minimum distance between the model and the wall during the test. Integrating the ΔC_P over the surface of the model would result in a change in normal force of less than 0.2 percent.

The vortex lattice solution is in agreement with the experimental results in showing negligible wall interference.

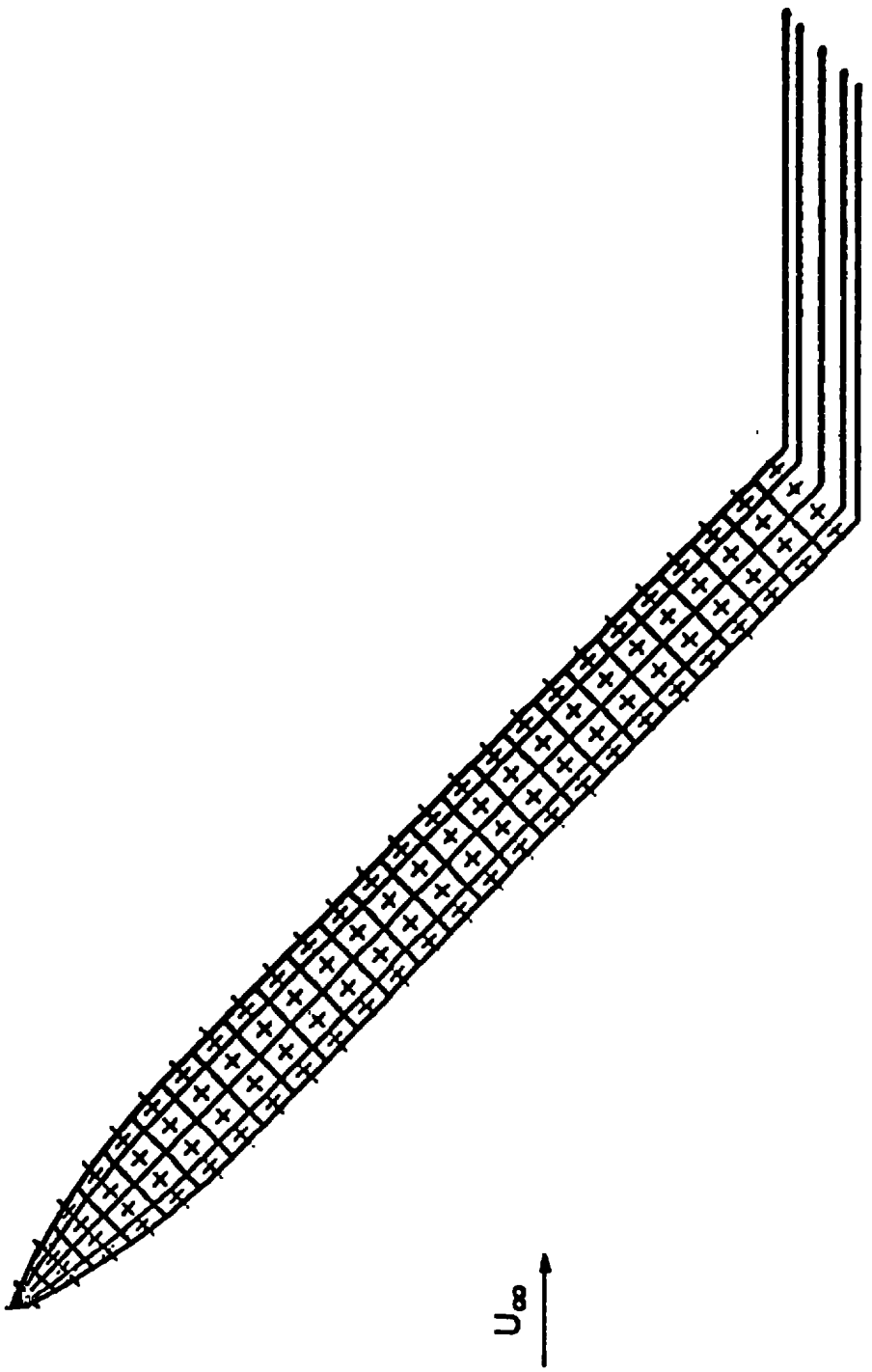

Figure B-1. Vortex lattice model of missile body.

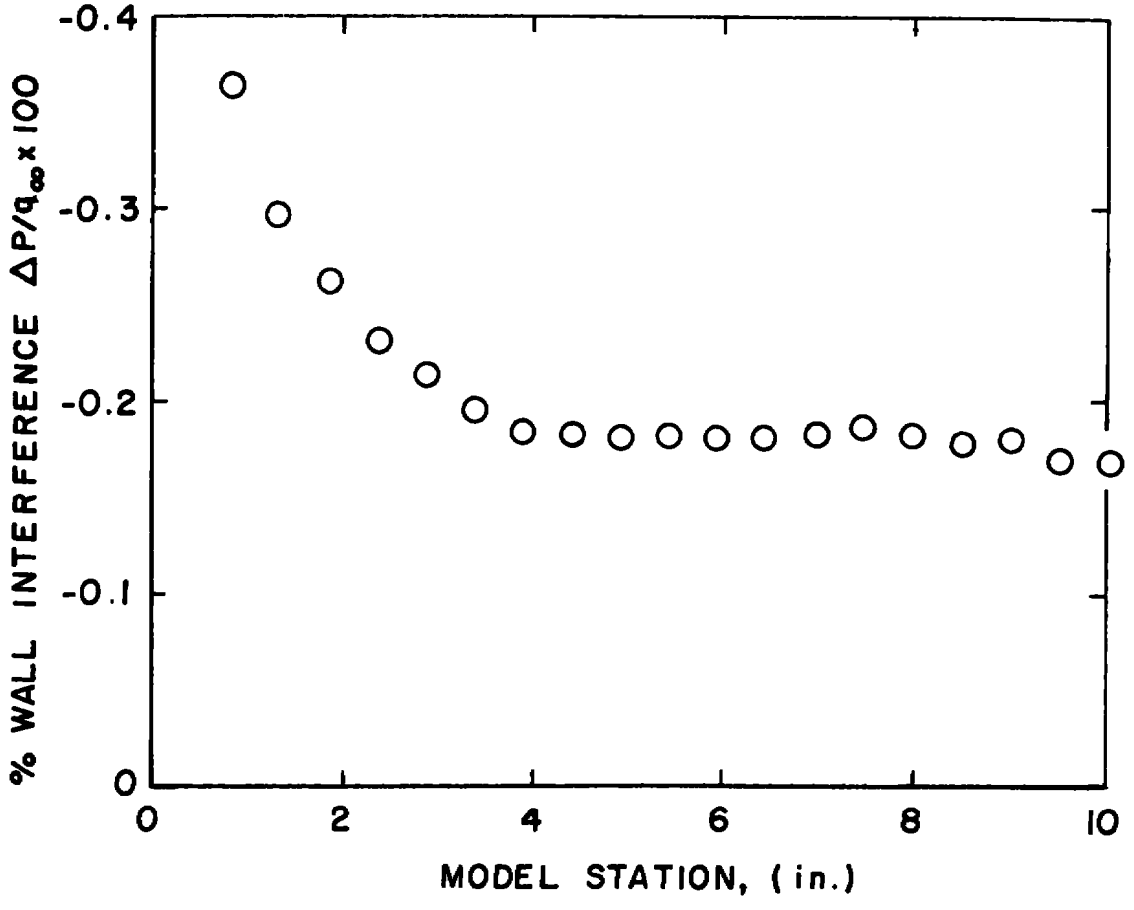

Figure B-2. Computed wall interference.

NOMENCLATURE

C_{D_N}	Crossflow drag coefficient for an infinite cylinder, normal force/$q_\infty S$
C_m	Pitching-moment coefficient, pitching moment about a point 6.25 in. from model nose/$q_\infty Sd$
C_N	Normal-force coefficient, normal force/$q_\infty S$
C_p	Pressure cofficient, $(p - p_\infty)/q_\infty$
d	Model diameter, in.
ℓ	Model length, in.
M	Free-stream Mach number
p	Pressure
q_∞	Free-stream dynamic pressure
Re	Free-stream Reynolds number
S	Model cross-sectional area, $\pi d^2/4$
S_b	Model base area, in.^{2}
S_p	Model planform area, in.^{2}
X_{CP}	Center-of-pressure location, in model diameters, from moment reference center, CLM/CN